https://doi.org/10.5194/egusphere-2024-3720
Preprint. Discussion started: 19 December 2024

Comparative ozone production sensitivity to NO_x and VOCs in Quito, Ecuador and Santiago, Chile: implications for control strategies in times of climate action

María Cazorla[1], Melissa Trujillo[1], Rodrigo Seguel[2,3], Laura Gallardo[2,3]

[1]Universidad San Francisco de Quito USFQ, Instituto de Investigaciones Atmosféricas, Quito, Ecuador
[2]Center for Climate and Resilience Research (CR2), Universidad de Chile, Santiago, Chile
[3]Departamento de Geofísica, Facultad de Ciencias Físicas y Matemáticas, Universidad de Chile, Santiago, Chile

Correspondence to: María Cazorla (mcazorla@usfq.edu.ec)

Abstract. Amid the current climate crisis, cities are being called to reduce levels of atmospheric pollutants that are short-lived climate forcers (SLCF) such as ozone and $PM_{2.5}$. This endeavor presents new challenges in terms of control strategies. Here, we scrutinize the ozone production sensitivity to NO_x and VOCs in Quito, Ecuador and Santiago, Chile, and we discuss the implications for precursor controls. To this end, we use a chemical box-model constrained with VOCs, meteorological, and air quality data. Comparable ozone production rates ($P(O_3)$=15-35 ppbv h^{-1}) were found to influence both cities, which lead to a well-established ozone season in Santiago, but not in Quito. A partial explanation to this difference is the distinct mixing conditions in both cities. Alkenes and aromatics contribute 60-90% to ozone production in Quito and 50-60% in Santiago. Aldehydes and ketones contribute an additional 20-30% in Santiago. Isoprene contributes 10% in Quito and 20% in Santiago. Any isolated measure to reduce NO_x alone would impact both cities negatively. For example, a 75 % reduction in NO_x causes a 30% increase in peak $P(O_3)$ in Quito and a 54% increase in Santiago. In contrast, equal reductions in NO_x and VOCs would have a beneficial effect. For example, a 75% decrease in both precursors would cut the peak $P(O_3)$ by more than half in both cities. Therefore, only parallel controls on NO_x and VOCs in both cities have the potential of curbing ozone from the simultaneous perspective of public health and climate action.

1. Introduction

Tropospheric ozone bears a dual nature of a serious air contaminant and a short-lived climate forcer (SLCF). At the ground level, ozone negatively impacts the health of human and non-human populations due to its oxidative nature that affects the respiration function in living beings (Karlsson et al., 2017; Madden and Hogsett, 2001; Malley et al., 2017; Soares and Silva, 2022). Furthermore, tropospheric ozone is the third largest anthropogenic climate forcer (Anon, 2014; Checa-Garcia et al., 2018), and it deters carbon sinks as it is a limiting factor to carbon capture in vegetation (Mills et al., 2016; Zhang et al., 2022). Hence, mitigating the ozone abundance in the ambient air is an action that simultaneously protects public health while combats climate change. For this reason, cities are currently called to take this action (Intergovernmental Panel on Climate Change (IPCC), 2023). In most cities across the world, ozone is considered one of the criteria air pollutants and thus is regulated by local and national legislation (Lyu et al., 2023). However, ozone continues to be a major air quality concern in many regions despite decades of studying the complex and non-linear nature of its production chemistry. This complexity imposes tailoring control strategies appropriate for each city that carefully consider the local makeup of the ambient air.

The mitigation of ozone to benefit in parallel air quality and climate presents a new challenge in devising efficient controls on ozone precursors at the urban level. This need is particularly pressing in regions that are highly vulnerable to climate change and

https://doi.org/10.5194/egusphere-2024-3720
Preprint. Discussion started: 19 December 2024

that still struggle with poor air quality, such as cities in South America (SA) (Cazorla et al., 2022). In this work, we scrutinize the chemistry of ozone production and its sensitivity to its precursors (NO_x and VOCs) in a comparative fashion between Quito (Ecuador) and Santiago (Chile). To this end, we present a unique set of VOC measurements taken in Santiago in March 2021. We use VOC vs. CO correlations from measurements in Santiago to scale CO and estimate VOCs in Quito. We incorporate VOCS, meteorological, and air quality data into a detailed photochemical box model using the F0AM (Framework for 0-D Atmospheric Modeling) (Wolfe et al., 2016). We present a discussion about the impact of changing precursor proportion on the chemistry of ozone production at both cities that could result from actions meant to curb ozone as an air pollutant and a SLCF.

A recent ozone trend study in South America demonstrated that the short- and long-term ozone exposure in tropical cities Quito and Bogota are lower than those encountered at extratropical cities Santiago and São Paulo (Seguel et al., 2024). This regional distribution of ozone exposure seems somewhat counterintuitive, given year-round solar radiation at high altitudes over tropical Andean cities combined with their intense traffic emissions. Previous work showed that a VOC-limited environment constrained ozone production in Quito, but rates of ozone production were not compared to other cities in the region (Cazorla, 2016). On the other hand, Santiago has been dealing with over two decades of ozone pollution and seasonal exceedances that are worsening in time due to an increased frequency of extreme wildfire events (Seguel et al., 2020, 2024). In this work we compare the ozone production chemistry between both cities to gain insight into mechanisms that can lead to ozone accumulation in the ambient air.

An important angle to this work is investigating what would be the effect of applying control measures to reduce levels of air pollutants that are SLCFs on ozone production rates. For example, many cities in SA, including Quito and Santiago, have a seasonal high $PM_{2.5}$ problem (Gómez Peláez et al., 2020). As with ozone, reducing levels of $PM_{2.5}$ in cities protects public health while it is an effective climate action (Intergovernmental Panel on Climate Change (IPCC), 2023). A direct way of cutting down levels of $PM_{2.5}$ is reducing diesel-based traffic emissions, which in turn lowers NO_x levels. This beneficial outcome was observed during the COVID-19 pandemic confinements, when primary pollutants and $PM_{2.5}$ decreased immediately as a direct consequence of mobility restrictions. However, the effect on ozone was the opposite. Research conducted in Quito, Santiago and other South American cities proved that NO_x reductions increased ozone production rates and ambient ozone due to a shift in the production chemistry from a VOC-limited towards a more NO_x-limited regime (Cazorla et al., 2021b; Seguel et al., 2022; Sokhi et al., 2021). Another example worth-noting is a modeling study in the city of Cuenca, Ecuador, that showed how the sole measure of replacing the diesel-based public transportation by electric means would decrease $PM_{2.5}$ and NO_2, but the levels of ambient ozone would increase (Parra and Espinoza, 2020). These eye-opening results impose a need to assess the impact of shifting the composition of precursors on the ozone forming chemistry that could arrive from applying controls on individual contaminants. It follows that assessing combined changes in both sets of precursors (NO_x and VOCs) is critical, which we present in this work.

With the above motivations, we employ a comparative approach to the chemistry of ozone formation in Quito and Santiago to address the following research questions:

a) How do the typical magnitudes of ozone production rates compare between Quito and Santiago? Thus, what are likely reasons that explain ozone levels in the ambient air in both cities?
b) What chemical groups of VOCs contribute the most to ozone production in each city?
c) What would be the effect on ozone production if drastic reductions in NO_x, VOCS or both were enforced in each city?

https://doi.org/10.5194/egusphere-2024-3720
Preprint. Discussion started: 19 December 2024

In the Methods section, we briefly describe ozone chemistry and the way we calculate ozone production and loss rates as well as radical production rates. Furthermore, we provide details of the study sites, time periods, and data sets. In addition, we give a full explanation of model details, constraints, and runs. In the Results and Discussion section, we compare pollutant levels, magnitudes of ozone production rates, radical abundances, and radical production rates between both cities. In addition, we quantify the contribution of different VOC groups to ozone production, and we discuss ozone production rates under different scenarios of NO_x and VOCs. In the Conclusions section we present the main findings, and we emphasize the adverse or favorable implications of adopting specific control strategies on ozone precursors at both cities.

2. Methods

2.1 Ozone and radical production and losses

The abundance of ozone in the ambient air is the result from a balance between chemical production, chemical loss, dry deposition, and ozone transport due to advection (Seinfeld and Pandis, 2016). Sometimes, stratospheric intrusions could also contribute to the ozone budget (Archibald et al., 2020). The net chemical production rate, denoted as $P(O_3)$ in this study, (instantaneous chemical production minus chemical loss), is a direct source of ozone in the ambient air. Under atmospheric stability conditions, $P(O_3)$ is the culprit for ozone accumulation within the mixing layer. The chemistry of ozone production has been studied extensively for several decades (Gery et al., 1989; Haagen-Smit and Fox, 1956; Kleinman, 2005a; Logan et al., 1981; Thornton et al., 2002a). A simplified mechanism is depicted in reactions R1-R8. The hydroxyl radical, OH, oxidizes VOCs and leads to the formation of the hydroperoxyl radical, HO_2, and other peroxy- radicals, RO_2 (R1). The latter two react with fresh emissions of NO, which produces NO_2 (R2, R3). From these reactions, OH and other organic radicals (RO) are formed. The photolysis of NO_2 with daylight splits the molecule into ground state oxygen, O, and reforms NO (R4). Subsequently, O rapidly reacts with O_2, and ozone is formed (R5). Depending on the proportion of VOCs to NO_x, both sets of precursors compete to react with OH. Hence, OH and HO_2 radicals very rapidly cycle in a catalytic fashion to feed the mechanism with new NO_2 that undergoes photolysis and forms ozone. The titration of NO by ozone (R6) is not a real ozone sink during daytime due to the rapid NO_2 photolysis. From this mechanism, the rate equation for the instantaneous chemical production of ozone (p) is derived from reactions R2 and R3, as is depicted in equation (1) (Ren et al., 2013; Seinfeld and Pandis, 2016; Shirley et al., 2006; Thornton et al., 2002b).

$OH + VOC \rightarrow HO_2, RO_2 + H_2O$ (R1)

$HO_2 + NO \rightarrow NO_2 + OH$ (R2)

$RO_2 + NO \rightarrow NO_2 + RO$ (R3)

$NO_2 + hv \rightarrow O + NO$ (R4)

$O + O_2 \rightarrow O_3$ (R5)

$O_3 + NO \rightarrow NO_2 + O_2$ (R6)

$OH + NO_2 + M \rightarrow HNO_3 + M$ (R7)

$HO_2 + HO_2 \rightarrow H_2O_2 + O_2$ (R8)

$$p = k_{HO2+NO}[NO][HO_2] + \sum_i^n ki\,[NO][RO_2]_i \quad (1)$$

https://doi.org/10.5194/egusphere-2024-3720
Preprint. Discussion started: 19 December 2024

Meanwhile, ozone loss is driven by reactions that deplete radicals. In urban environments, the reaction of OH and NO_2 to form nitric acid (R7) is a main mechanism of ozone loss ((Seinfeld and Pandis, 2016; Sillman, 1995; Thornton et al., 2002b)). In the Quito and Santiago NO_x-rich environments R7 dominates in magnitude as we demonstrate in the Results section. Other ozone losses, such as the reaction of O_3 with HO_2 or the reaction of alkenes and O_3, yield loss rates two orders of magnitude lower than the loss to nitric acid, while the reaction of O^1D with water vapor yields rates an order of magnitude lower. Hence, for practical purposes, we calculate the net ozone production rate $P(O_3)$ using (2).

$$P(O_3) = k_{HO2+NO}[NO][HO_2] + \sum_i^n ki\,[NO][RO_2]_i - k_{OH+NO2+M}[OH][NO_2][M] \quad (2)$$

Previous studies show that the formation of nitric acid (R7) or hydrogen peroxide (R8) can be used as indicators of the chemical regime of ozone production (Kleinman, 2005a; Kleinman et al., 2001a; Sillman, 1995). In a VOC-limited regime, HO_x radicals are lost due to reactions with NO_x with R7 being a well-known chemical fate. In a NO_x-limited regime, reactions between HO_x radicals (collectively OH and HO_2) have been identified as an important chemical loss. For example, the reaction between two HO_2 radicals produces hydrogen peroxide, H_2O_2 (R8). The equations to quantify these two main radical losses are depicted as L_1 and L_2 in equations (3) and (4).

$$L_1 = k_{OH+NO2+M}[OH][NO_2][M] \quad (3)$$

$$L_2 = 2k_{HO2+HO2}[HO_2]^2 \quad (4)$$

In this work, we use the ratio L1/(L1+L2) as an indicator of the chemical regime of ozone production (Kleinman, 2005b; Kleinman et al., 2001b). Thus, ratios greater that 0.5 indicate that radical losses to the production of nitric acid dominate, which takes place in a VOC-limited (NO_x-saturated) regime, while ratios below 0.5 indicate that reactions among radicals, such as R8, are important and mark a shift towards the NO_x-limited regime.

With respect to the production of HO_x, we include the main atmospheric sources of OH and HO_2 to calculate radical production rates, $P(HO_x)$. Thus, reactions (R9) to (R11) briefly depict ozone photolysis followed by the reaction of O^1D with water vapor, which produces OH radicals (Levy, 1971). Other important sources of OH and HO_2 in the urban atmosphere are the photolysis of HONO and formaldehyde (R12 and R13) (Dusanter et al., 2009; Ren et al., 2013). Therefore, equations (5) to (7) were used to quantify these rates.

$$O_3 + hv \rightarrow O_2 + O^1D \quad (R9)$$

$$O^1D + M \rightarrow O + M \quad (R10)$$

$$O^1D + H_2O \rightarrow 2OH \quad (R11)$$

$$HONO + hv \rightarrow OH + NO \quad (R12)$$

$$HCHO + hv \rightarrow 2HO_2 \quad (R13)$$

$$P(HO_x)_1 = 2J_{O3\rightarrow O1D}[O_3]\, k_{(O1D+H2O)}[H_2O]/(k_{(O1D+M)}[M]) \quad (5)$$

$$P(HO_x)_3 = J_{HONO}[HONO] \quad (6)$$

$$P(HO_x)_2 = 2J_{HCHO}[HCHO] \quad (7)$$

https://doi.org/10.5194/egusphere-2024-3720
Preprint. Discussion started: 19 December 2024

2.2 Study sites and background information

A map with the location of the two study sites in Quito, Ecuador, and Santiago, Chile is shown in Fig. 1. Details of the stations chosen for the study as well as background information follow.

One of the sites is located at Universidad San Francisco de Quito's Atmospheric Measurement Station (EMA USFQ, Spanish Acronym) at coordinates 0.19°S, 78.43°W, and 2414 m a.s.l. Quito (2.78 million inhabitants) is an Andean city at high altitude where meteorological conditions fluctuate within rainy and dry seasons. The times of the year with increased precipitation peak around March and November, while the drier months run from July to mid-September (Cazorla et al., 2024). However, very sunny conditions can develop any time of the year in this equatorial city, especially during the March and September equinoxes. A discussion on weather patterns that influence air quality in Quito can be found in previous work (Cazorla and Juncosa, 2018).

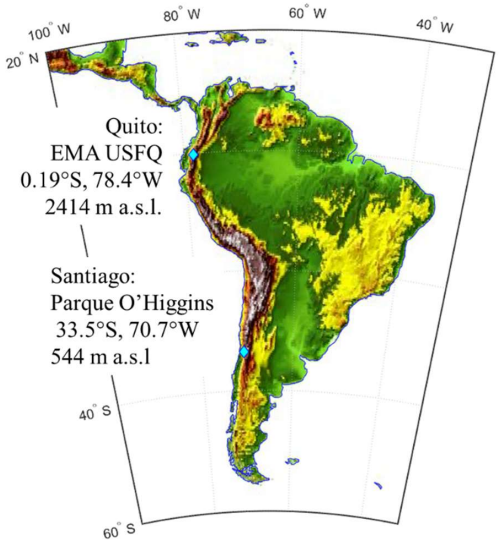

Figure 1. Map of South America with location and coordinates of EMA USFQ station in Quito, Ecuador and Parque O'Higgins station in Santiago, Chile.

In Santiago, we chose Parque O'Higgins station, located in the center of the city, at coordinates 33.46°S, 70.66°W, and 535 m a.s.l. This station is run by the Ministry of the Environment, and it typically represents the city's average conditions (Osses et al., 2013). Santiago, (8 million inhabitants) is a subtropical city influenced by four seasons. The warmest and sunniest months take place during the austral summer (December to February), but the high ozone season often extends until March. March is an interesting month in terms of air quality in Santiago because high temperatures and insolation prevail, while anthropogenic emissions and ozone precursors increase as the school year starts and the flow of people into the city increases.

https://doi.org/10.5194/egusphere-2024-3720
Preprint. Discussion started: 19 December 2024

2.3 Study time periods

2.3.1 March 2021

A field campaign to measure VOCs in Santiago was conducted in March 2021 (description in section 2.4.2 and Appendix A). Therefore, we performed detailed modeling of the chemistry of ozone production for mostly sunny days during March 2021 in both cities. We filtered out overcast days because photolysis frequencies were not measured and, thus, we rely on modeled actinic flux without cloud cover correction for the photolysis component of the model. March 2021 was mostly sunny in Santiago, so only 5 days were filtered out, while 11 days were filtered out for Quito. Fig. S1 in the supplementary information shows the time series of solar radiation at both cities overlapping mostly sunny days to all days.

2.3.2 Mean conditions by season (Santiago) or month-grouping (Quito) in 2022

To further explore ozone production under additional precursor conditions that are typically observed within a year in each city, we run simulations for average conditions in 2022 by season (Santiago) or month-grouping (Quito). For Santiago, we run the model for a typical sunny day in austral summer (February only because data in January was of poor quality), fall (March to May), winter (June to August), and spring (September to November). Mean conditions were found by overlapping meteorological and air quality data (1-hour resolution) in 24-hour plots and finding the average for every hour, namely the mean diurnal variation (MDV). These mean conditions were used as model input to run the model. Model input variables are described in section 3.

In Quito, the amount of daylight as well as environmental conditions do not vary much within a year due to its equatorial latitude. Thus, we sampled average conditions in several months along 2022. We run simulations for a typical sunny day in January, often a sunny month; June-July, a time with low precursors due to summer vacation; September, an equinox month with increased pollution due to resuming school traffic; and October-November, a time of transitioning into the rainy season. Mean conditions for each period were found in a similar way as it was done for Santiago.

2.4 Data

2.4.1 Ozone, NO, NO_2, CO, and meteorological data

Santiago

Air quality data and meteorological conditions (1-hour) measured at Parque O'Higgins station were obtained from the Air Quality National Information System maintained by the Ministry of Environment (SINCA, Spanish acronym, https://sinca.mma.gob.cl/). From network information, ozone is measured with UV photometry, NO_x with chemiluminescence, CO with infrared photometry, and published data complies with quality control standards according to national legislation (https://sinca.mma.gob.cl/index.php/documentos). Fig. S2 (Supplement) depicts a time series of measurements in March 2021. For comparisons with Quito, the time coordinate in all figures in this work are presented in UTC-5 (local and solar time in Quito and roughly solar time in Santiago).

All data described in this section is available as complete input files for the F0AM model (see data availability statement).

Quito

Ozone is measured at EMA USFQ with a Thermo 49i UV photometer. Measurements are periodically intercompared against a 2B-Technologies UV photometer. The agreement between measurements is better than 5%. A Teledyne 400 chemiluminescence instrument is used to measure NO-NO_2-NO_x. Calibration is done with a certified NO standard and zero air to prepare calibration mixtures. Uncertainty in measurements is better than 5% (Cazorla, 2016). The original rate of acquisition of ozone and NO_x

https://doi.org/10.5194/egusphere-2024-3720
Preprint. Discussion started: 19 December 2024

measurements is 1-second. Meteorological measurements are also available at EMA USFQ with an original rate of acquisition of 30-second. CO is not measured at EMA USFQ. However, the car fleet is similar in the entire city. Hence, following previous work (Cazorla et al., 2021b), we used an average of CO measurements from three stations (Belisario, Centro and Tumbaco) run by the Quito Air Quality Network (Secretariat of the Environment, Quito, Ecuador) (https://aireambiente.quito.gob.ec/). Fig. S3 depicts a time series of Quito observations.

2.4.2 VOCs

Santiago

VOC measurements in Santiago were taken from a fourth-story window at the Geophysics Department of Universidad de Chile (33.457 ºS, 70.662 ºW, 535 m a.s.l.) from 17 to 28 March 2021, corresponding to the late summer. The site is located at campus Beauchef, in downtown Santiago, at 770 m from Parque O'Higgins station, where ozone, carbon monoxide, nitrogen oxides, and meteorological parameters are measured.

VOCs were measured using PTR-TOF-MS (proton transfer reaction time of flight mass spectrometry) at 1-minute resolution. The instrument used was an Ionicon Analytik GmbH, Model 1000. A detailed description of the sampling technique, technical operation of the PTR-TOF-MS instrument, calibration and mass discrimination methodology as well as the limit of detection of measured compounds is given in Appendix A. Table 1 shows the parent molecules utilized in this study. Grouping was done for the practical purpose of organizing model runs, as explained in Section 2.5. In Appendix B (Fig. B1), we present the time series of measured VOCs. Based on details in Appendix A, we estimate a conservative error of 30-40% in all VOC observations.

Measurements of VOCs were linearly correlated to CO observations and these correlations were used to derive VOCs in Santiago for the days of March when VOCs were not measured. The same technique was used to derive VOCs for a typical day per season in 2022. Linear correlations were obtained with 1-hour data. Table 1 shows the correlation parameters of the linear fit. Correlations for compounds associated to traffic (10 cases) show R^2>0.83 and correspond to alkenes, aromatics, and some oxygenated compounds (methanol, ethanol, and phenol). Some of the latter compounds could also have a biogenic origin, but finding exact proportions from each source was not within the scope this study. High correlation between traffic-borne VOCs and CO has also been reported in previous studies (Bon et al., 2011). The correlation is less good for other oxygenated compounds, namely acetaldehyde and acetic acid (R^2=0.61). R^2 is the lowest for formaldehyde and acetone (R^2 = 0.34 and 0.35), which we attribute to the secondary nature of these compounds. As expected, isoprene does not correlate well (R^2 = 0.47) for being a biogenic compound. However, monoterpenes do (R^2=0.82), for which we partially associate these compounds with traffic sources in addition to biogenic sources. Thus, in the case of compounds that do not relate directly to CO, determination coefficients are low. However, we use the same scaling technique to derive the abundance of these compounds on days when measurements were not available until better estimates become available.

Quito

Measurements of VOCs are unavailable in Quito. Thus, we scaled local CO observations using the linear correlations found at Santiago (Table 1). In previous work (Cazorla et al., 2021b), VOCs for Quito were estimated from VOC/CO ratios extracted from previous work conducted in Mexico City (Jaimes-Palomera et al., 2016). The VOC/CO ratios (slope of linear fit) found at Santiago for propene is similar (0.008) to the one found at Mexico City (0.0076), but greater for toluene by 34% (0.0076 vs.

https://doi.org/10.5194/egusphere-2024-3720
Preprint. Discussion started: 19 December 2024

0.005), benzene by 53.7% (0.0026 vs. 0.0012), and ethylbenzene by 97% (0.0159 vs 0.00045). These are the only coincident compounds between both studies. We regard the current VOC estimations for Quito as an improvement because the Santiago measurements are more recent, have a more complete set of compounds, and because of our direct access to data and methodology. Nevertheless, we acknowledge the uncertainty of estimating VOCs and the need for a new iteration of this study whenever in situ measurements of VOCs become available in Quito. From the available information (differences with the Mexico study and the error in the Santiago measurements), we estimate a conservative uncertainty of 50-60% for VOCs in Quito, but further studies need to refine this estimate.

Table 1. VOCs measured in Santiago from 17 to 28 March 2021 and linear correlations of VOCs vs. CO in ppbv .

Group	Species	Slope × 10^{-3}	Intercept	R^2
Aromatic compounds traffic-associated	Benzene	2.60	-0.88	0.86
	Toluene	7.61	-3.02	0.89
	Ethylbenzene	15.93	-6.65	0.83
	Styrene	0.97	-0.25	0.86
	C-9 Aromatics	3.67	-1.50	0.89
Alkenes traffic-associated	Propene	7.56	-2.56	0.87
	Butene	9.78	-3.19	0.83
Biogenic	Isoprene	0.81	0.31	0.47
Biogenic or traffic-related	Monoterpenes	0.65	-0.14	0.82
Oxygenated Alcohols	Methanol	19.87	-5.35	0.86
	Ethanol	4.89	-2.26	0.86
	Phenol	0.99	-0.02	0.84
	Cresol	0.20	0.22	0.27
Oxygenated Aldehydes and ketones	Formaldehyde	0.95	1.06	0.34
	Acetaldehyde	12.65	-1.47	0.61
	Acetone	5.38	2.34	0.35
	Butanone	4.78	-1.41	0.72
	Methacrolein_MVK (Methyl Vinyl Ketone)	0.90	0.19	0.74
	Acetic Acid	15.16	-2.54	0.61

2.5 Model details

We used the F0AM (Wolfe et al., 2016) to model ozone formation chemistry in Quito and Santiago in March 2021 and for average conditions per season (Santiago) or month-grouping (Quito) in 2022. The chemical mechanistic information was taken from the Master Chemical Mechanism, MCM v3.3.1 (Bloss et al., 2005; Jenkin et al., 1997, 2003, 2015; Saunders et al., 2003), via website: www.mcm.york.ac.uk. The F0AM is a model that runs in MATLAB (https://la.mathworks.com/). We used

https://doi.org/10.5194/egusphere-2024-3720
Preprint. Discussion started: 19 December 2024

MATLAB R2024a licensed to USFQ. We provide open data sources for model input (see Data Availability). Details of model settings, and simulations follow.

2.5.1 Model input

We constrained the model with ozone, NO, NO_2, CO, and meteorological observations from both cities. VOC observations in Santiago and estimations in Quito were also used to constrain the model. The time step for the March 2021 model runs was 10 minutes. To this end, original Quito data were integrated into 10-minute resolution. The same was done with Santiago 1-minute VOC data. Regarding air quality and meteorological observations in Santiago, 1-hour data were linearly interpolated to generate 10-minute time series. In contrast, the 2022 runs were done using 1-hour data for average conditions in a season (Santiago) or month-grouping (Quito).

For the VOC input, measurements were distributed among primary VOCs available in the MCM using equal weighing for all compounds. For example, compounds measured as butanone/butanal were distributed as 50% butanone and 50% butanal. These correspond to MCM notations MEK and C_3H_7CHO, respectively. Table S1 in the Supplement shows all VOC compounds organized by chemical groups with the measurement nomenclature and with the weighting factors attributed to explicit MCM compounds. Thus, a total of 35 VOCs were input to the model. Compound-grouping and notation used in this study, along with all input species are depicted in Table 2.

Table 2. VOCs measured in Santiago, Chile in March 2021 and used as model input.

Group	Notation	Compounds
Alkenes	ALK	1-butene, cis-butene, trans-butene, propene
Aromatics	ARO	benzene, toluene, styrene
		ethylbenzene, o-xylene, m-xylene, p-xylene
		propylbenzene, cumene, 1,2,3-trimethylbenzene, 1,2,4-trimethylbenzene, 1,3,5-trimethylbenzene, 2-ethyltoluene, 3-ethyltoluene, 4-ethyltoluene
Oxygenated	OXY	methanol, ethanol, phenol, cresol
	ALD	formaldehyde, acetaldehyde, acetic acid
		acetone, propanal, methacrolein, methyl ethyl ketone, butanal
Biogenic	ISO	isoprene
		alpha-pinene, beta-pinene, limonene

Frequencies of photolysis were modeled using the MCM option in the F0AM for both cities. In the Results section we compare the mean diurnal variation of JNO_2 and JO^1D between both cities and with previous studies.

For the ozone column and albedo inputs in the F0AM, we used 1-hour area-averaged MERRA-2 (Modern-Era Retrospective analysis for Research and Applications, Version 2) data sets for Quito and Santiago (Global Modeling and Assimilation Office (GMAO), 2015a, b). This data selection was based on previous work that showed good performance of MERRA-2 products for total column ozone in the region (Cazorla and Herrera, 2022a).

https://doi.org/10.5194/egusphere-2024-3720
Preprint. Discussion started: 19 December 2024

Table S2 contains a summary of options chosen in the F0AM for model runs.

2.5.2 Model runs and scenarios

The model components to this study consist of a base run, VOC sensitivity runs, anthropogenic precursor scenario runs, and isoprene scenario runs (Table 3). These simulations were done comparatively for both cities with the March 2021 data. Table 3 presents details of the model runs, notation, and factors applied to precursor concentrations in each case. Notation is consistent with VOC groups in Table 2. The base run includes all measured VOC compounds. Subsequently, for the VOC sensitivity portion, we computed the individual percentage contribution to ozone production by each VOC group. Furthermore, we run sensitivity scenarios decreasing NO_x alone and together with VOCs by 75%, 50% and 25%. The purpose of running these scenarios is to evaluate the impact of applying potential isolated controls on NO_x versus applying simultaneous controls to NO_x and VOCs. In addition, we run isoprene scenarios, which are relevant from the perspective that isoprene is emitted by vegetation as a protection to biotic and abiotic stresses, a mechanism that might be enhanced in a drying and warming climate (Arneth et al., 2010). This aspect is of particular relevance for Santiago given the expected impacts of climate change in this region (Boisier et al., 2018). Thus, we simulated scenarios of increasing and decreasing isoprene alone by 100% and 50%, and increasing isoprene by 100% while decreasing NO_x by 50%. Results are discussed in section 3.

Finally, we applied the base run to typical conditions per season (Santiago) or month-grouping (Quito) to investigate ozone production rates under other conditions observed within a year in both cities. Thus, four runs were applied to 2022 seasonal conditions for each city, as described in 2.2.2.

Table 3. Model runs and factors used to modify precursor concentrations

Study Component	Notation	Factors used on precursor concentrations							
		NO	NO_2	CO	ALK	ARO	OXY	ALD	ISO
Base run	ALK+ARO+OXY+ALD+ISO	1	1	1	1	1	1	1	1
VOC Sensitivity	ALK	1	1	1	1	0	0	0	0
	ALK+ARO	1	1	1	1	1	0	0	0
	ALK+ARO+OXY	1	1	1	1	1	1	0	0
	ALK+ARO+OXY+ALD	1	1	1	1	1	1	1	0
Anthropogenic Precursor Scenarios	75% NO_x decrease	0.25	0.25	1	1	1	1	1	1
	50% NO_x decrease	0.50	0.50	1	1	1	1	1	1
	25% NO_x decrease	0.75	0.75	1	1	1	1	1	1
	75% NO_x&VOCs decrease	0.25	0.25	0.25	0.25	0.25	0.25	0.25	1
	50% NO_x&VOCs decrease	0.50	0.50	0.50	0.50	0.50	0.50	0.5	1
	25% NO_x& VOCs decrease	0.75	0.75	0.75	0.75	0.75	0.75	0.75	1
Isoprene Scenarios (*)	100% Isoprene increase	1	1	1	1	1	1	1	2
	50% Isoprene decrease	1	1	1	1	1	1	1	0.50
	100% Isoprene increase & 50% NO_x decrease	0.50	0.50	1	1	1	1	1	2

(*) Only isoprene was modified.

https://doi.org/10.5194/egusphere-2024-3720
Preprint. Discussion started: 19 December 2024

3 Results and discussion

3.1 March 2021

3.1.1 Air pollutant levels

Ozone maxima in Santiago ranged between 30 to below 70 ppbv in March 2021, as shown by percentiles 10 and 90 of diurnal profiles obtained with 1-hour data in Fig. 2a. Looking at the entire data set, half of the days in the month had ozone higher than 50 ppbv and there was a day with a maximum of 100 ppbv on March 4 (the school year started on March 1). Unlike Santiago, Quito does not have a well-established ozone problem or season, despite equatorial solar radiation at high altitude and urban emissions. Usually, 1-hour data remain below 50 ppbv. For example, in March 2021, ozone maxima during mostly sunny days ranged between 30 to 50 ppbv for percentiles 10 and 90 as depicted in Fig. 2a. In previous years, high ozone in Quito (usually up to 80 ppbv) has been recorded episodically and has been associated with wildfires in the surrounding forests, usually during the month of September (Cadena et al., 2021).

Regarding levels of NO_x, ambient concentrations of NO and NO_2 in Santiago in March 2021 were larger than in Quito by a factor of 3 for the maximum at the 50th percentile, as depicted in Fig. 2b and 2c. However, levels of CO were similar (Fig. 3d). The CO and NO diurnal profiles show strong signatures of the morning and evening rush hours over Quito. In contrast, the morning rush hour in Santiago stands out more, while the evening signature is delayed and less prominent.

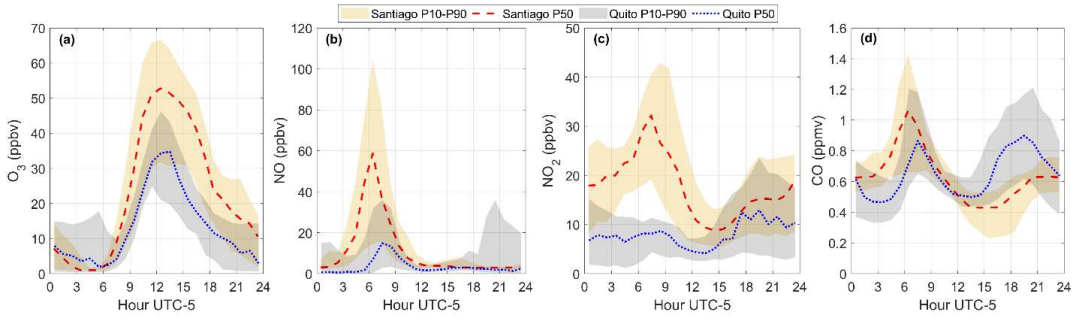

Figure 2. Diurnal variation of a) ozone, b) NO, c) NO_2, and d) CO for Santiago and Quito in March 2021. The red dashed line is the diurnal variation for Santiago at the 50th percentile and the dotted blue line is the same but for Quito. Orange shadow is limited at the bottom and top by the 10th and 90th percentile diurnal variations of every variable for Santiago. The gray shadow is the same but for Quito.

The diurnal NO_2-to-NO_x ratio shows some similarities between the two cities, particularly between noon and 15:00 (Fig. 3). This ratio is a good indicator of photochemical activity involving nitric oxide (NO) reacting with hydroperoxyl (HO_2) and alkyl peroxy radicals (RO_2), leading to the production of NO_2. However, in Santiago, this ratio increases one and a half hours earlier than in Quito, which indicates active photochemistry since the early morning in Santiago that continues into the afternoon.

https://doi.org/10.5194/egusphere-2024-3720
Preprint. Discussion started: 19 December 2024

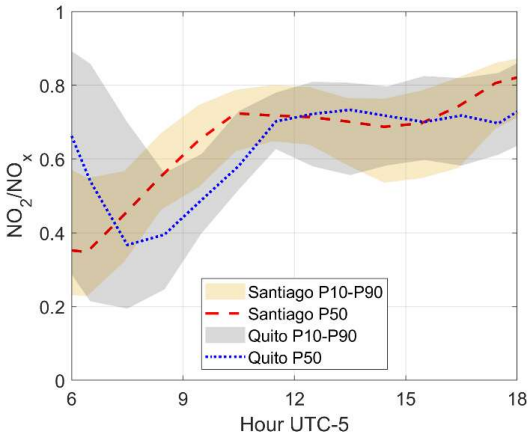

Figure 3. Diurnal variation of the NO_2/NO_x ratio at the 50th percentile for Santiago (red dashed line) and Quito (blue dotted line) in March 2021. Shadows depict limits at the 10th and 90th percentiles at Santiago (orange) and Quito (gray).

3.1.2 Base run

JO^1D and JNO_2

Photolysis reactions are key to radical and ozone production during daylight hours. Being Quito and Santiago located on the equator and in the subtropics, respectively, the magnitude of frequencies of photolysis are different due to the intensity of solar radiation at both locations. From model output, the diurnal variation at the 50th percentile of frequencies of photolysis of ozone (towards the production of O^1D) and NO_2 in March 2021 are presented in Fig. 4. As expected, both quantities are greater in Quito than in Santiago for its equatorial location and high altitude. Previous work on the oxidation capacity of the Santiago air reported direct measurements of JO^1D and JNO_2 taken during a field campaign in March 2005 (Elshorbany et al., 2009a). These measurements for diurnal maxima in Santiago were $JNO_2 \sim 0.008$ and $JO^1D \sim 2.5x10^{-5}$ s^{-1}, which are similar to mean values obtained through modeling in this work (Fig. 4).

https://doi.org/10.5194/egusphere-2024-3720
Preprint. Discussion started: 19 December 2024

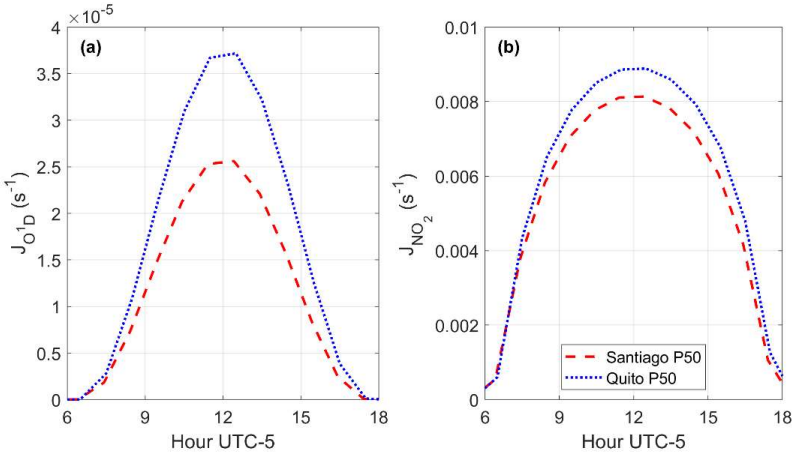

Figure 4. Comparison between the diurnal variation of frequencies of photolysis a) JO^1D and b) JNO_2 in Quito and Santiago at the 50th percentile.

OH, HO_2, RO_2, and rates of radical production

Radical abundances in both cities during the study time period are illustrated in Fig. 5. With higher frequencies of photolysis, the OH abundance in Quito is overall larger than in Santiago (Fig. 5a). This is evident from the Quito diurnal profile at the 50th percentile in Fig. 5a and close packing of data within percentiles 10 and 90 that contrast with Santiago. Maximum abundances at the 50th percentile are 0.25 and 0.22 pptv in Quito and Santigo, respectively. The order of magnitude of radical abundances is similar to those found in other studies (Cazorla et al., 2021b; Dusanter et al., 2009; Ren et al., 2013).

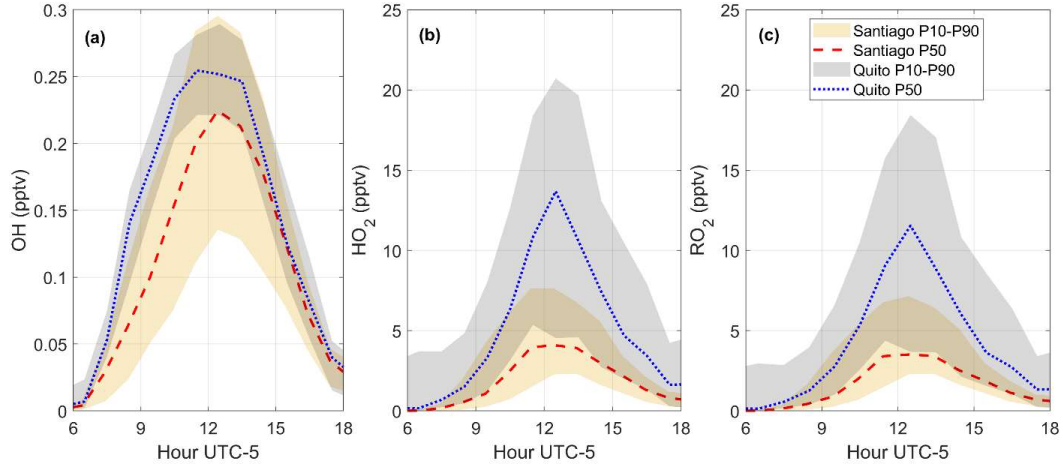

Figure 5. Diurnal variation of a) OH, b) HO_2, and RO_2 in Quito and Santiago at the 50th percentile (blue dashed line and red dotted line, respectively). Shadows indicate limits set by the 10th and 90th percentiles (orange for Santiago and gray for Quito).

https://doi.org/10.5194/egusphere-2024-3720
Preprint. Discussion started: 19 December 2024

The main source of OH is the photolysis of ozone followed by the reaction of O^1D with water vapor. The diurnal maximum of radical production rate from this source (percentile 50) is about 1 pptv s^{-1} in both cities with Quito values being slightly larger (Fig. 6a). From meteorological data, the water vapor content at solar noon in Quito is about 10 g kg^{-1}, while in Santiago is about 9 g kg^{-1}, but JO^1D is greater in Quito. Due to high altitude, Quito is a city with rather low humidity in spite of its tropical latitude. Furthermore, at Santiago data scattering is larger than in Quito as it happens with the OH abundance. Given that the OH availability is larger in Quito, reactions with VOCs yield HO_2 and RO_2 abundances about three times greater in Quito than in Santiago (Fig. 5b and 5c). From the magnitudes in the latter figures, HO_2 and RO_2 are equallly important, which is consistent with previous work (Bottorff et al., 2023; Dusanter et al., 2009; Elshorbany et al., 2009a).

In the morning, radical production from the photolysis of HONO is equally important in Santiago and in Quito (0.28 pptv s^{-1}), as indicated in Fig. 6b, which is expected at rich NO_x environments. However, the contribution from this radical source in Santiago gradually decreases from the mid-morning into the afternoon, while it drops sudenly at noon in Quito (Fig. 6b). This difference indicates higher photochemical activity in the morning in Quito and less in the afternoon. Formaldehyde photolysis as a source of radicals is greater in Santiago, especially at noon and in the afternoon (Fig. 6c). However, this is a less important source when its magnitude is compared to the magnituede of the two other sources. Previous work determined $P(HO_x)$ from different sources in Santiago (Elshorbany et al., 2009a). Thus, Elshorbany et al. found rates of HO_2 production from formaldehyde photolysis that are about 60% higher (0.15 ppt s^{-1}, on average) than the magnitudes found in this study. Furthermore in the aforementioned study, rates of OH production from HONO photolysis are about 30% higher (0.4 ppt s^{-1}, on average), while rates of OH production from ozone photolysis are substantially lower (0.27 ppt s^{-1}, on average) . These differences are due to lower abundances of measured formaldehyde and modeled HONO in this study than the abundances reported in Elshorbany's 2005 study. For example, the latter reports mean HONO and formaldehyde levels up to 4 and 7 ppbv, respectively. Meanwhile, in this study, the diurnal maximum of formaldehyde is 2 ppbv (percentile 50, from measurements) and 0.4 ppbv for HONO (percentile 50, from model output).

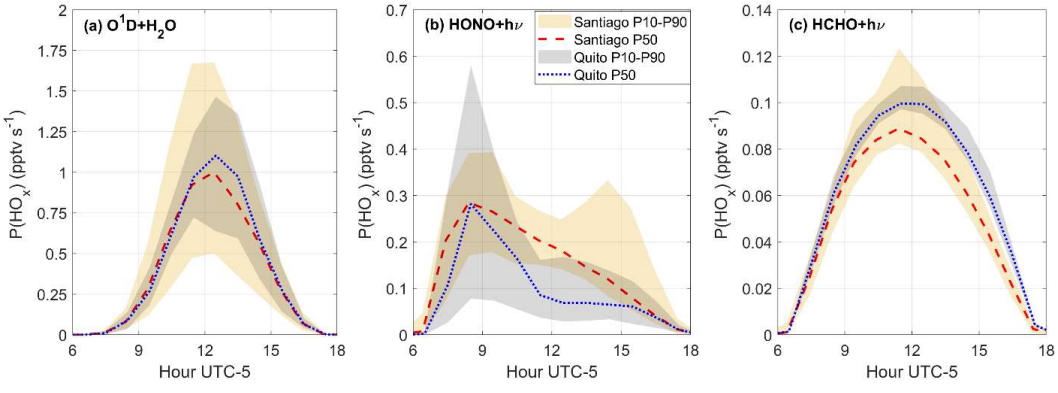

Figure 6. Diurnal variation of radical sources: a) ozone photolysis followed by $O^1D + H_2O$, b) HONO photolysis, and c) formaldehyde photolysis in Quito and Santiago at the 50th percentile (blue dashed line and red dotted line, respectively). Shadows indicate limits set by the 10th and 90th percentiles (orange for Santiago and gray for Quito).

https://doi.org/10.5194/egusphere-2024-3720
Preprint. Discussion started: 19 December 2024

Ozone production and loss

Magnitudes of ozone production rates at both cities are comparable for the 50th percentile diurnal profile (maximum of about 22-23 ppbv h^{-1}), but the time of the maximum shifts towards the morning over Quito (Fig. 7a and 7b). This is consistent with more active photochemical production of radicals, for example from HONO photolysis in the morning hours (Fig. 6b). The range of values within percentiles 10 and 90 (about 15 to about 35 ppbv h^{-1}) is also comparable. In Quito, the HO_2 and RO_2 abundance is greater when compared to Santiago, but NO levels are lower. Thus, there is a compensating effect in the levels of HO_2 and NO in both cities in a way that application of equation (1) yields about similar ozone production rates. Previous work that determined net ozone production rates in Santiago from measurements and model calculations in 2005, reported substantially higher values for the mean $P(O_3)$ diurnal maximum (160 ppb h^{-1}) (Elshorbany et al., 2009b). This value seems high, although it is possible that after almost twenty years of reassessing $P(O_3)$ in Santiago, conditions changed. However, the mean $P(O_3)$ maximum presented in Fig. 7a is consistent with values of mean diurnal maximum of $P(O_3)$ obtained from direct measurements and photochemical modeling, for example in Houston in 2009 (~30 ppb h^{-1}) (Cazorla et al., 2012). Likewise, a recent sensitivity study of ozone production to NO_x and VOCs in New York City (Sebol et al., 2024), that uses the F0AM model, reported a $P(O_3)$ range of 26-37 ppb h^{-1}, which is similar to our results.

The chemical regime of ozone production in Santiago is strongly VOC-limited as indicated by the loss rate to the production of nitric acid, depicted in Fig. 7b. These rates are 2 to 3 times greater in Santiago than in Quito. This finding is consistent with the loss rate to the formation of hydrogen peroxide being greater in Quito than in Santiago (Fig. 7c), although the magnitude of this loss is an an order of magnitud lower than losses to nitric acid at both cities.

As stated earlier, the ratio L1/(L1+L2), where L1 is the loss to the formation of nitric and L2 is the loss to hydrogen peroxide, is a common way to assess the VOC-limited character of the chemistry of ozone production. In the case of Quito, the chemical regime is also VOC-limited as L1/(L1+L2) at the 50th percentile is between 0.9 and 1 as shown in Fig. 8a (solid black line). However, this chemical character is more intense at Santiago as this ratio lays very close to 1 (Fig. 8b). This finding illustrates that within the VOC-limited and NO_x-limited categories of ozone production lay a range of intensities that depend on the unique conditions that surround every urban area. In the following sections we explore scenarios that have the potential to shift this strong chemical character at each city.

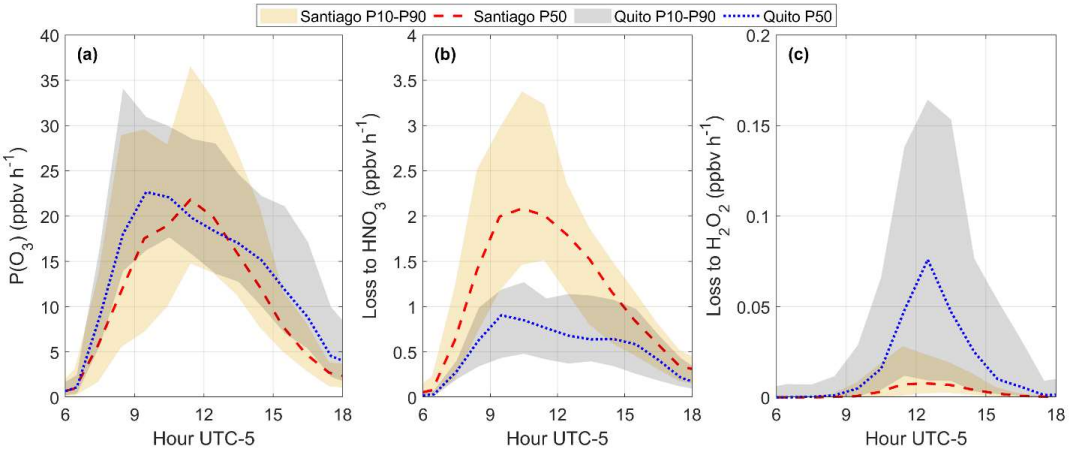

https://doi.org/10.5194/egusphere-2024-3720
Preprint. Discussion started: 19 December 2024

Figure 7. Diurnal variation of a) Net ozone production, b) Loss to nitric acid, and c) Loss to hydrogen peroxide in Quito and Santiago at the 50th percentile (blue dashed line and red dotted line, respectively). Shadows indicate limits set by the 10th and 90th percentiles (orange for Santiago and gray for Quito).

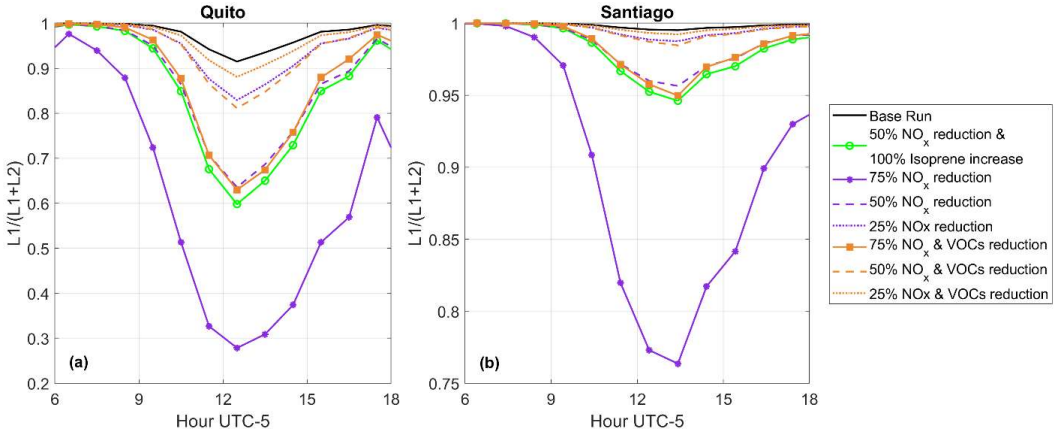

Figure 8. Diurnal variation of losses to nitric acid to total losses (nitric acid and hydrogen peroxide) as L1/(L1+L2) for a) Quito and b) Santiago at the 50th percentile. Overlapping curves correspond to model runs as detailed in Table 3 and figure legend.

Ozone production and ambient ozone

Our model simulations indicate that at both cities high photolysis frequencies and sufficient precursor availability set the right conditions for comparable radical and ozone production rates. However, $P(O_3)$ of like magnitudes are associated to ozone levels in Quito that are lower than in Santiago. A partial explanation to this fundamental difference lays in the vertical mixing conditions that dominate both cities. Santiago has a year-round influence of the Subtropical Pacific High that determines a strong subsidence inversion, which is often strengthen by low-level lows and occasionally disrupted by passing synoptic disturbances (Gallardo et al., 2002; Garreaud et al., 2002; Huneeus et al., 2006; Muñoz and Undurraga, 2010). Such meteorological conditions are known to be the cause of pollutant accumulation in the boundary layer in Santiago. In Quito, circulation patterns that affect air quality are less studied and characterized, partially due to the topographic complexity of the region. However, there is experimental evidence of strong vertical mixing over the Quito region from the morphology of ozone vertical profiles studied over the past ten years (Cazorla, 2017; Cazorla et al., 2021a; Cazorla and Herrera, 2022b). Additionally, previous studies demonstrate that on sunny days in Quito, a deep convective boundary layer develops in connection with thermal and mechanical eddies that break the early morning thermal inversion (Cazorla and Juncosa, 2018; Muñoz et al., 2023). Thus, we propose that strong convection at this tropical area helps mix and dilute ozone produced at the surface in the vertical direction. Future studies need to incorporate chemical transport models to simulate ozone aboundances under different vertical mixing scenarios. In addition, other chemical fates of ozone precursors that lead to photochemical fractions different from ozone need to be further explored.

In spite of limitations, from this modeling work we identified that average $P(O_3)$ magnitudes of 23 ppbv h^{-1} (or higher) combined with well-known meteorological conditions produce seasonally elevated levels of ambient ozone over Santiago. In contrast, the

https://doi.org/10.5194/egusphere-2024-3720
Preprint. Discussion started: 19 December 2024

same average $P(O_3)$ magnitudes over Quito are associated to ambient ozone that usually meets the national air quality standard (51 ppbv). The question remains as per what magnitudes of $P(O_3)$ are high enough in Quito to power down mixing conditions and overshoot normal ambient ozone levels. Shifting ozone precursors permanently as a result of changes in environmental policy that controls atmospheric pollutants could cause unwanted changes towards higher ozone production rates. As countries and cities are urged to implement climate actions that curb fossil fuel use, changes in environmental policy are expected to happen at some point in the future. In upcoming sections we quantify the impact of changing ozone precursor abundance on the magnitude of ozone production rates.

3.1.3 VOC sensitivity

Ozone production sensitivity to VOCs in both cities was evaluated by determining the contribution to $P(O_3)$ by individual chemical groups as defined in Table 2. Diurnal profiles of $P(O_3)$ at the 50th percentile, when one VOC group at a time is added to the model, are presented in Fig. 9a (Quito) and 9b (Santiago). With only alkenes, $P(O_3)$ maxima in Quito and Santiago reach 12 and 9 ppbv h^{-1}. Adding aromatic compounds more than doubles ozone production rates in the morning over Quito (from 7 to about 16 ppbv h^{-1} at 09h00). Also, there is a shift towards more active photochemistry earlier in the day as the $P(O_3)$ maximum is displaced from noon (12 ppbv h^{-1}) to the mid-morning (18 ppbv h^{-1}). In Santiago, the addition of aromatics increases the $P(O_3)$ maximum from 9 to 14 ppb h^{-1}, but there is no change in the time of peak $P(O_3)$. Oxygenated compounds (only alcohols and excluding aldehydes and ketones) practically do not cause an increase in ozone production rates in Santiago, while there is a negative effect over Quito mainly in the mid-morning. In contrast, adding aldehydes and ketones causes an additional increase in the morning $P(O_3)$ in Quito and shifts the maximum even earlier (up to 21 ppbv h^{-1}). In Santiago, this group increases $P(O_3)$ throughout the day and the maximum up to almost 19 ppbv h^{-1}. These results are consistent with previous findings in regard to alkenes, aromatics, and aldehydes being important contributors to ozone production (Bowman and Seinfeld, 1994; Calvert et al., 2000; Fanizza et al., 2014). Finally, the addition of isoprene causes an additional increase of $P(O_3)$ in Quito in the mid-morning to the early afternoon. Over Santiago, the effect of isoprene is important from the morning to the afternoon, bringing the $P(O_3)$ maximum up to 22 ppb h^{-1}. This last run also contains monoterpenes, but they do not cause a visible effect in $P(O_3)$ for which they are not shown as a separate curve.

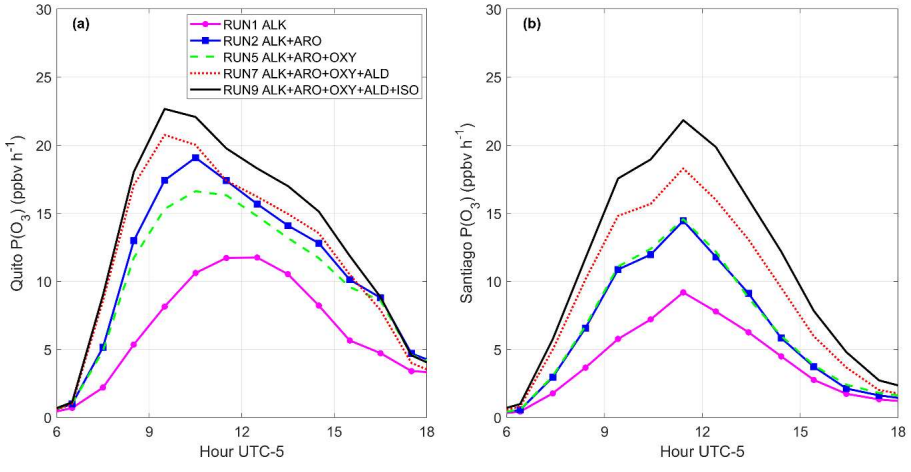

Figure 9. Diurnal variation of net ozone production at the 50th percentile when individual VOC groups are added to the model run according to grouping in Table 2 for a) Quito, and b) Santiago.

https://doi.org/10.5194/egusphere-2024-3720
Preprint. Discussion started: 19 December 2024

The percentage increase in $P(O_3)$ caused by every chemical group during daylight hours at both cities is depicted in Fig. 10a (Quito) and 10b (Santiago). Alkenes and aromatics combined (blue and cyan in Fig. 10a) produce 60 to 90% of $P(O_3)$ in Quito with the lower contribution at around 07h00 and the higher contribution mostly before noon and into the afternoon. Meanwhile, the contribution of these two groups to $P(O_3)$ in Santiago is 50-60% throughout the day. The contribution of aldehydes and ketones is substantial over Santiago, which combined with alkenes and aromatics make up for 80-90% $P(O_3)$ during daylight hours (magenta in Fig. 10b). In Quito, aldehydes and ketones are only important in the morning, between 07h00-08h00, when the percentage contribution could be up to 30%. Isoprene contributes an additional 10-20% in Santiago and becomes increasingly important towards the afternoon, while in Quito this contribution is about 10%. However, this contribution is affected by error as the isoprene abundance in Quito was estimated (CO scaling) as opposed to measured for which it needs further research. Oxygenated compounds (alcohols) only affect $P(O_3)$ marginally in Santiago, while in Quito these compounds slightly lower $P(O_3)$. As in the case of isoprene, this contribution could also be affected by greater error.

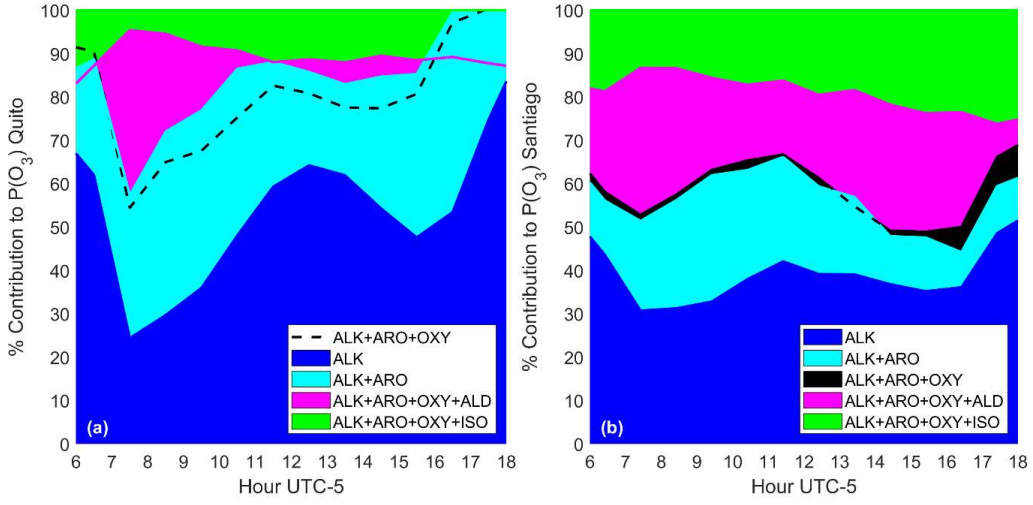

Figure 10. Percentage contribution to $P(O_3)$ by chemical groups at a) Quito and b) Santiago.

3.1.4 NOx and VOC scenarios

Environmental action directed to improving air quality and climate demand applying control strategies to reduce levels of atmospheric pollutants. As stated before, diesel-based public transportation in South American cities is an important source of $PM_{2.5}$ and NO_x that, in turn, is also associated to the formation of $PM_{2.5}$. Having this in mind, we explore the consequences of reducing this type of transportation as it is often included in air quality and climate mitigation planning. Notice that Santiago's public transport bus fleet has roughly 10% of electric buses, a fraction that is expected to increase in the future.

The impact of applying controls only on NO_x are quantified in Fig. 11. The scenarios investigated were those of NO_x reductions in 25%, 50%, and 75%. In Quito, a 25% decrease in NO_x causes a modest $P(O_3)$ increase in the morning (Fig. 11a), but a 50% reduction shifts faster ozone production rates before 09h00. A 75% decrease in NO_x causes a substantial increase in morning ozone production rates, but at noon the chemical regime shifts to NO_x-limited and ozone production drops. The evolution of the chemical regime shifting towards NO_x-limited in Quito from the first scenario (25% NO_x reduction) to the third (75% NO_x reduction) is illustrated in Fig. 8a. In the third scenario, the ratio L1/(L1+L2) drops below 0.5, which indicates that losses to

https://doi.org/10.5194/egusphere-2024-3720
Preprint. Discussion started: 19 December 2024

hydrogen peroxide become increasingly important from before noon into the afternoon. Meanwhile in Santiago, the greater the NO_x reduction, the higher the ozone production rates during daylight hours (Fig. 11b). A 75% reduction in NO_x causes the ozone production maximum to increase by a factor of 1.8, while for the 50% reduction the factor is 1.4. In the third scenario, faster ozone production maxima shift before noon for both cases. With a 75% reduction in NO_x there is a visible departure of the ozone formation chemistry towards a less VOC-limited regime, although the L1/(L1+L2) ratio is still below 0.5 (Fig. 8b).

The former simulations demonstrate that lowering solely NO_x has a harmful effect in Santiago and Quito. As increased ozone production rates contribute to the overall ozone budget, this isolated measure should be avoided in both cities due to the potential risk of exceeding current ambient ozone levels.

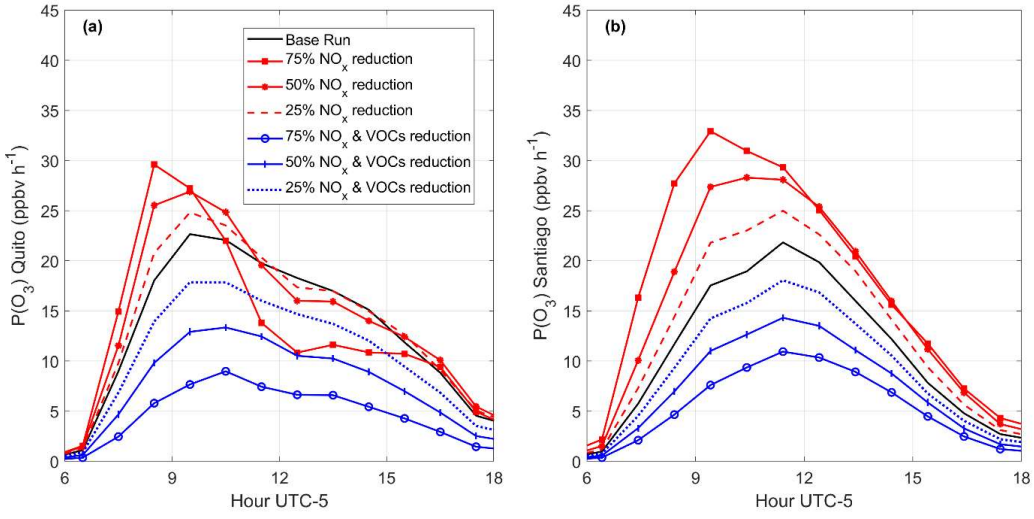

Figure 11. Diurnal variation of net ozone production at the 50th percentile for model scenarios detailed in Table 4 (legend) for a) Quito, and b) Santiago.

In contrast, reducing VOCs along with NO_x, has a positive effect in all tested scenarios (equal reductions by 25%, 50%, and 75%), as presented in Fig. 11a and 11b. Thus, ozone production rates could drop by more than 50% if all precursors were to rapidly drop by 75%. An example of this scenario would be the quick and massive decarbonization of the transportation sector, both gasoline and diesel-based, which would reduce VOCs and NO_x. This measure would improve air quality and help climate action because the two most important urban pollutants that are also SLCF, ozone and $PM_{2.5}$, would decrease in the ambient air. More modest reductions in both sets of precursors also would resonate with beneficial effects as shown in Fig. 11. In this work we applied equal reduction factors to NO_x and VOCs, but future work needs to further investigate the proportion in VOC to NO_x reduction when controls are applied to emissions from mobile sources as well as specific reductions per type of VOC.

In the case of isoprene, model runs show that doubling or reducing isoprene concentrations by half only causes a modest increase or decrease in $P(O_3)$, as presented in Fig. S4. On the other hand, if NO_x is reduced by half, while isoprene is doubled, $P(O_3)$ increases to levels close to those caused by a reduction of NO_x by 50% (Fig. 11 and Fig. S4). Thus, the most important driver of change is a change in NO_x when compared to a change in isoprene alone. However, previous studies demonstrate that isoprene is highly reactive and that VOC-limited environments are prone to faster $P(O_3)$ when isoprene increases (Sebol et al., 2024).

https://doi.org/10.5194/egusphere-2024-3720
Preprint. Discussion started: 19 December 2024

Therefore, our results need to be further investigated with extended isoprene measurements and modeling in the future, particularly due to the climate sensitivity of isoprene emissions and the climate mitigation pathways to be adopted (Saunier et al., 2020).

3.2 Mean conditions by season

As per additional conditions observed within a year in Quito and Santiago, Fig. 12 illustrates the range of mean levels of O_3, NO, NO_2, and CO that are typical in both cities (2022 data). In Quito, the daily ozone maxima progressively range from 30 to 45 ppbv, with higher ozone levels in September and lower in June-July (Fig. 12a). In contrast, Santiago data show clear seasonal differences in data distribution with mean summer peak ozone concentrations being more than 2.5 times higher than those of the winter (20 vs 55 ppbv) (Fig. 12b). The diurnal cycles shown in Fig. 12 are smoothed out when hourly data are averaged within a season. However, when inspecting 1-hour time series, only on 1 day in 2022 ozone was higher than 60 ppbv in Quito. Meanwhile in Santiago, the peak ozone values were between 60-100 ppbv in 48 days. Table S3 shows statistics for 2022 data in both places.

Regarding NO, peak values in the diurnal cycle in Quito range between 30 to 55 ppbv, but there are times in the year when NO spikes substantially in the rush hour (Fig. 12c). In 2022, this spike happened in October-November. In Santiago, NO is substantially higher in the winter months (Fig. 12d). As temperatures are low, the mixing volume remains shallow and primary pollutants such as NO accumulate, while the actinic flux is not sufficient to activate photochemistry. In the 1-hour time series, 148 days in 2022 had NO higher than 100 ppbv in Santiago, while in Quito there were 31 days with morning NO of such magnitudes.

In Santiago, the winter-to-summer variability is also evident in the diurnal cycles of NO_2 and CO, with higher concentrations during the cold months (Fig. 12e and 12g). In contrast, the variability is small in Quito for NO_2, especially during daylight hours, and marginal for CO (Fig. 12f and 12).

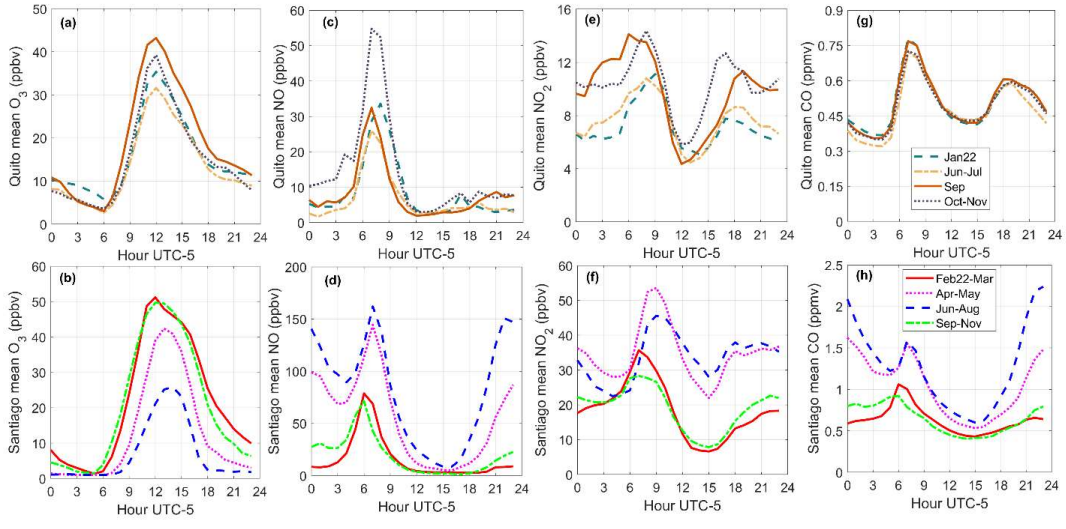

Figure 12. Air quality conditions observed within a year by season (Santiago) or month-grouping (Quito) presented comparatively for a) and b) ozone, c) and d) NO, e) and f) NO_2, and g) and h) CO.

https://doi.org/10.5194/egusphere-2024-3720
Preprint. Discussion started: 19 December 2024

With the range of conditions presented in Fig. 12, the range of ozone production rates expected on average in both cities is depicted in Fig. 13a (Quito) and 13b (Santiago). Thus, over Quito the mean ozone production rates roughly range from 15-25 ppbv h^{-1} year-round, which is comparable to observed rates during the ozone season in Santiago (summer). However, differences in ambient ozone levels point to physical mixing conditions as a partial explanation. Other chemical paths for precursors, for example to the production of nitrate particles or PAN, need to be further explored in Quito as a potential chemical reason in addition to the physical explanation that we propose in this study.

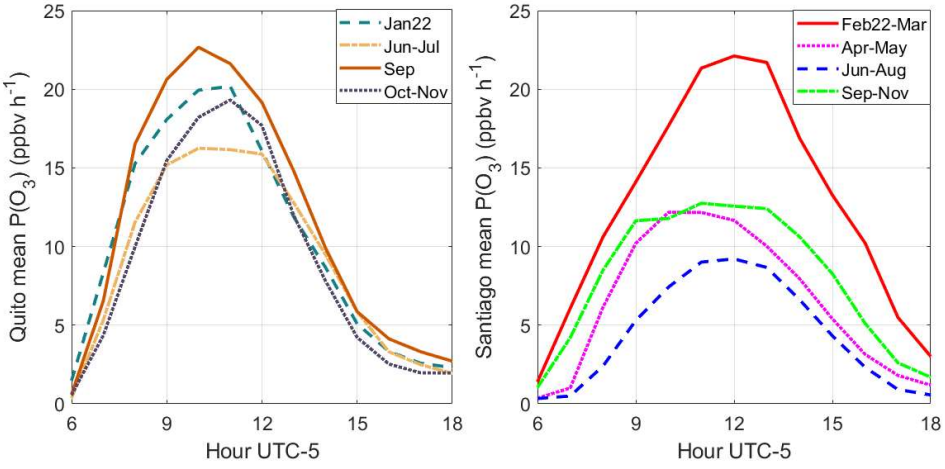

Figure 13. Comparison of the range of net ozone production rates observed in a year (2022) in a) Quito and b) Santiago.

4 Conclusions

Ozone production rates in Quito and Santiago were calculated using the F0AM (Framework for 0-D Atmospheric Modeling), a chemical box model, constrained by a unique set of VOC measurements taken in Santiago in March 2021. For Quito, the model was constrained using VOCs derived by scaling CO with experimental VOC vs. CO linear correlations found in Santiago. From model results, Quito and Santiago are VOC-limited environments influenced by comparable rates of ozone production. On sunny days, these rates are about 23 ppbv h^{-1}, on average, but the range is 15-35 ppbv h^{-1}. However, these magnitudes of $P(O_3)$ do not result in comparable ambient ozone at both cities as ozone is greater in Santiago. This result seems counterintuitive being Quito an equatorial city at high altitude with plentiful solar radiation and urban emissions. Santiago has a well-known ozone season that takes place in the austral summer (December to February) but extends into March. For example, in March 2021 there were 11 days in Santiago when 1-hour ozone observations were between 60-80 ppbv and one day when ozone was 101 ppbv. Meanwhile in Quito, 1-hour data stayed below 50 ppbv the entire month. In 2022, 13% of 1-hour observations in Santiago were between 60-90 ppbv, while in Quito only 1 day in 2022 surpassed 60 ppbv. We partially attribute this fundamental difference to physical reasons related to mixing conditions at both cities, but chemical reasons need to be further explored. Thus, it is well-documented that Santiago's air quality is permanently impacted by the Subtropical Pacific High, which causes a strong subsidence inversion. This circumstance, together with the magnitudes of ozone production rates identified in this work, lead to ozone accumulation in the ambient air. On the other hand, there is observational evidence that the vertical mixing is strong over Quito. Thus, we propose that although ozone is produced at fast rates in Quito, it quickly becomes mixed vertically at this highly

https://doi.org/10.5194/egusphere-2024-3720
Preprint. Discussion started: 19 December 2024

585 convective tropical environment. Future studies need to verify this hypothesis with chemical transport models. Also, additional research is needed to explore other chemical fates of precursors to form photochemical fractions other that ozone in Quito.

As in the case of ozone production rates, radical production rates are comparable at both cities, on average. From ozone photolysis radical rates are about 1 pptv s^{-1}; from HONO photolysis 0.28 pptv s-1; and from formaldehyde photolysis 0.08 to 0.1 pptv s^{-1}. However, ozone production rates of like magnitudes result from a compensating effect in the magnitude of radical
590 abundance relative to NO abundance. Thus, the abundance of HO_2 and RO_2 radicals is greater in Quito than in Santiago (about 13 pptv for each set of radicals versus 4 pptv, on average) but NO is two to three times greater in Santiago. Given the latter, the VOC-limited character of the ozone production chemical regime is much more intense over Santiago although the Quito environment is also VOC-limited.

As per the chemical nature of VOCs that contribute the most to the formation of ozone, alkenes and aromatics contribute in 60-
595 90% over Quito, while in Santiago these two groups contribute with about 60% and aldehydes and ketones with an additional 30%. The contribution of isoprene is about 10% in Quito, and between 10 and 20% in Santiago, but additional research is needed to further investigate isoprene sensitivity in both environments.

Due to the current climate crisis and ongoing decline of environmental conditions, currently cities have been called to reduce fossil fuel use and, therefore, SLCF. As per changes in environmental policy that could be implemented as simultaneous
600 measures to benefit climate and protect public health, it is of major relevance to state that any isolated strategy to reduce NO_x alone will result in a harmful increase of net ozone production rates at both cities. For example, a 75 % reduction in NO_x would raise peak ozone production by 30% in Quito and 54% in Santiago. In contrast, equal reductions in NO_x and VOCs, even if modest, will decrease net ozone production rates. For example, a 25% decrease in both sets of precursors would result in a beneficial 20% reduction in peak ozone production rates at both cities. A more drastic reduction of a 75% decrease would cut
605 peak ozone production rates by more than half in both cities. Therefore, only parallel controls on NO_x and VOCs in both cities have the potential of curbing ozone from the simultaneous perspective of public health and climate action.

Appendix A: VOC measurements in Santiago, Chile

VOCs were measured by a PTR-TOF-MS (Ionicon Analytik GmbH, Model 1000). Ambient air was drawn with an external pump (KNF, N86KN.18) through a sampling line (1/8''). The sample air was injected into the PTR from a T-union via a polyether-ether-
610 ketone (PEEK) capillary (1/16'') conditioned at 80 ºC. The ion source was supplied with a 15 cm^3 min^{-1} water vapor flow. The drift tube was operated at temperature, voltage and pressure of 353 K, 600 V and 2.3 mbar, respectively, corresponding to a reduced electric field strength (E/N ratio) of ~136 Td (Townsend) (1 Td =10-17V cm^2).

The mass scale was calibrated every 10 minutes using H_3O+ isotope (21.0220), NO+ (29.9970) and protonated acetone (59.0490), while the voltage of the multichannel plate detector was optimized weekly. The relative mass discrimination (transmission) was
615 calculated before the campaign using a calibration gas standard and known reaction rates. The limit of detection (LoD) was calculated as three times the standard deviation of the background signal from zero air measurements (ENVEA, Model ZAG7001). We use a certified gas standard traceable to NIST (National Institute of Standards and Technology) for calibration checks for benzene (79.054), toluene (93.070), and ethylbenzene+xylenes (107.086). The error for toluene, ethylbenzene+xylenes, and benzene were -3%, -15% and +40%, respectively.

620 PTR-TOF-MS provides several advantages, including mass range and high measurement frequency. However, this technique is susceptible to fragmentation that may interfere at a given m/z. The data used in this work resulted from a series of field campaigns

https://doi.org/10.5194/egusphere-2024-3720
Preprint. Discussion started: 19 December 2024

aiming to optimize the measurements (e.g., E/N) and reduce the impact of fragmentation. We also used specific ion peaks collected by (Pagonis et al., 2019) in a public online library to identify reasonable VOC candidates in urban environments. Table 1 shows the protonated parent molecules detected in Santiago's atmosphere and the compound assigned by the monoisotopic m/z for identification. In general terms, PTR has been reported as a reliable way to measure species with higher proton affinities, such as aromatics (Table 1). However, m/z 107.086 produces fragments that interfere with m/z 79.054 (assigned to benzene), and therefore, a conservative error of 50% should be considered for benzene without known molecular fragmentation. We also detected interferences with m/z 69.070 (assigned to isoprene) during the morning rush hours. On the other hand, reactive species such as acetaldehyde, with high levels in Santiago, should be interpreted considering the photochemistry of Santiago. Table 1 also includes m/z values assigned to more than one species reported in the literature.

Table A1. Protonated parent molecules utilized in this study and VOCs assigned according to literature. More details can be found in Pagonis et al (2019) and in the PTR library. The table indicates names, parent ions and proton affinity obtained from https://webbook.nist.gov/chemistry/ and limit of detection.

Compound assigned	m/z	Proton affinity (kJ/mol)	Limit of Detection (ppbv)
Formaldehyde	31.018	712.9	1.0
Methanol	33.034	754.3	0.5
Propene/Cyclopropane	43.054	751.6/750.3	0.2
Acetaldehyde	45.033	768.5	0.4
Ethanol	47.049	779.4	0.5
1-Butene/2-Butene	57.070	-----	0.3
Acetone/Propanal	59.049	812/786	0.3
Acetic acid/Glycolaldehyde	61.028	783.7/N.A. [1]	0.4
Isoprene	69.070	826.4	0.2
Methacrolein/Methyl vinyl ketone	71.049	808.7/834.7	0.2
2-Butanone/Butanal	73.065	827.3/792.7	0.2
Benzene	79.054	750.4	0.09
Toluene	93.070	784.0	0.2
Phenol	95.049	817.3	0.2
Styrene	105.070	839.5	0.08
Ethyl benzene/Xylenes	107.086	-----	0.09
Cresol	109.065	N.A.	0.1
C_9-Aromatics	121.101	-----	0.05
Monoterpenes	137.132	-----	0.08

[1]N.A.: Not Available

https://doi.org/10.5194/egusphere-2024-3720
Preprint. Discussion started: 19 December 2024

Appendix B: Time series of VOCs measurements taken in Santiago

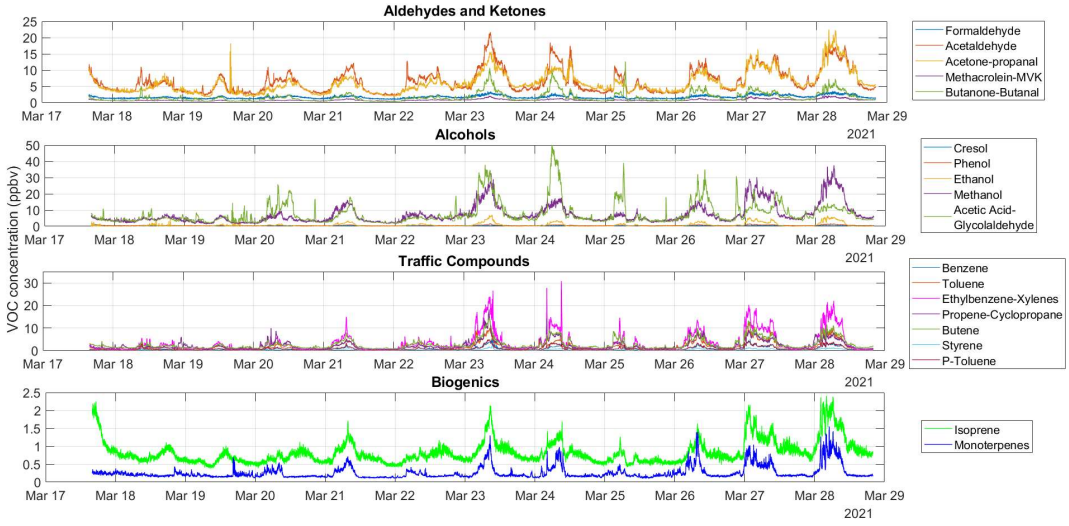

Figure B1. Time series (1-minute data) of VOCs measurements taken in Santiago, Chile from 17 to 28 March.

Data Availability

Complete input data files (soon to be generated DOI) (meteorology, air quality and VOCs) for the F0AM model base run (March 2021) for Quito and Santiago are available at: https://observaciones-iia.usfq.edu.ec/ under the folder 'Photochemical_Model_Quito_Santiago'.
Quito public air quality data can be accessed at: https://aireambiente.quito.gob.ec/
Santiago public air quality data can be accessed at: https://sinca.mma.gob.cl/
MERRA-2 total column ozone and albedo data can be found at: https://giovanni.gsfc.nasa.gov/giovanni/

Supplement

Separate document

Author contributions

MC, LG, RS: conceptualization. MC: model methodology. RS: VOC methodology. MT: data curation and model run. MC, MT: data analysis. MC: writing (original draft). All authors: writing, review and editing.

Competing interests

Authors declare not to have competing interests.

Acknowledgements

Thanks to Edgar Herrera and Lucas Castillo for their help at the beginning of this project. Thanks to Universidad San Francisco de Quito USFQ for their support during the development of this project. We acknowledge the use of public data from the Quito Air Quality Network (Secretariat of the Environment, Quito, Ecuador) and the National Air Quality Information System (Ministry of Environment, Chile).

https://doi.org/10.5194/egusphere-2024-3720
Preprint. Discussion started: 19 December 2024

Funding sources

This research was supported by Universidad San Francisco de Quito USFQ through Collaboration Grant 2022-2023.

References

Anon: Anthropogenic and Natural Radiative Forcing, in: Climate Change 2013 – The Physical Science Basis, Cambridge University Press, 659–740, https://doi.org/10.1017/CBO9781107415324.018, 2014.

Archibald, A. T., Neu, J. L., Elshorbany, Y. F., Cooper, O. R., Young, P. J., Akiyoshi, H., Cox, R. A., Coyle, M., Derwent, R. G., Deushi, M., Finco, A., Frost, G. J., Galbally, I. E., Gerosa, G., Granier, C., Griffiths, P. T., Hossaini, R., Hu, L., Jöckel, P., Josse, B., Lin, M. Y., Mertens, M., Morgenstern, O., Naja, M., Naik, V., Oltmans, S., Plummer, D. A., Revell, L. E., Saiz-Lopez, A., Saxena, P., Shin, Y. M., Shahid, I., Shallcross, D., Tilmes, S., Trickl, T., Wallington, T. J., Wang, T., Worden, H. M., and Zeng, G.: Tropospheric Ozone Assessment Report, Elementa: Science of the Anthropocene, 8, https://doi.org/10.1525/elementa.2020.034, 2020.

Arneth, A., Harrison, S. P., Zaehle, S., Tsigaridis, K., Menon, S., Bartlein, P. J., Feichter, J., Korhola, A., Kulmala, M., O'Donnell, D., Schurgers, G., Sorvari, S., and Vesala, T.: Terrestrial biogeochemical feedbacks in the climate system, Nat Geosci, 3, 525–532, https://doi.org/10.1038/ngeo905, 2010.

Bloss, C., Wagner, V., Jenkin, M. E., Volkamer, R., Bloss, W. J., Lee, J. D., Heard, D. E., Wirtz, K., Martin-Reviejo, M., Rea, G., Wenger, J. C., and Pilling, M. J.: Development of a detailed chemical mechanism (MCMv3.1) for the atmospheric oxidation of aromatic hydrocarbons, Atmos Chem Phys, 5, 641–664, https://doi.org/10.5194/acp-5-641-2005, 2005.

Boisier, J. P., Alvarez-Garreton, C., Cordero, R. R., Damiani, A., Gallardo, L., Garreaud, R. D., Lambert, F., Ramallo, C., Rojas, M., and Rondanelli, R.: Anthropogenic drying in central-southern Chile evidenced by long-term observations and climate model simulations, Elementa: Science of the Anthropocene, 6, https://doi.org/10.1525/elementa.328, 2018.

Bon, D. M., Ulbrich, I. M., de Gouw, J. A., Warneke, C., Kuster, W. C., Alexander, M. L., Baker, A., Beyersdorf, A. J., Blake, D., Fall, R., Jimenez, J. L., Herndon, S. C., Huey, L. G., Knighton, W. B., Ortega, J., Springston, S., and Vargas, O.: Measurements of volatile organic compounds at a suburban ground site (T1) in Mexico City during the MILAGRO 2006 campaign: measurement comparison, emission ratios, and source attribution, Atmos Chem Phys, 11, 2399–2421, https://doi.org/10.5194/acp-11-2399-2011, 2011.

Bottorff, B., Lew, M. M., Woo, Y., Rickly, P., Rollings, M. D., Deming, B., Anderson, D. C., Wood, E., Alwe, H. D., Millet, D. B., Weinheimer, A., Tyndall, G., Ortega, J., Dusanter, S., Leonardis, T., Flynn, J., Erickson, M., Alvarez, S., Rivera-Rios, J. C., Shutter, J. D., Keutsch, F., Helmig, D., Wang, W., Allen, H. M., Slade, J. H., Shepson, P. B., Bertman, S., and Stevens, P. S.: OH, HO_2, and RO_2 radical chemistry in a rural forest environment: measurements, model comparisons, and evidence of a missing radical sink, Atmos Chem Phys, 23, 10287–10311, https://doi.org/10.5194/acp-23-10287-2023, 2023.

Bowman, F. M. and Seinfeld, J. H.: Ozone productivity of atmospheric organics, Journal of Geophysical Research: Atmospheres, 99, 5309–5324, https://doi.org/10.1029/93JD03400, 1994.

Cadena, E., Daza, J., and Cazorla, M.: Eventos de ozono alto en Quito y sus precursores, in: Congreso Anual de Meteorología y Calidad del Aire CAMCA 2021. Available at: https://www.usfq.edu.ec/sites/default/files/2021-08/libro-abstracts-camca-2021.pdf (last access: 1 November 2024)., 2021.

Calvert, J. G., Atkinson, R., Kerr, J. A., Madronich, S., Moortgat, G. K., Wallington, , T J, and Yarwood, G.: Importance of Alkenes in the Chemistry of Ozone Generation in the Urban Atmosphere, in: The Mechanisms Of Atmospheric Oxidation Of The Alkenes, Oxford University PressNew York, NY, 3–22, https://doi.org/10.1093/oso/9780195131772.003.0001, 2000.

Cazorla, M.: Air quality over a populated andean region: Insights from measurements of ozone, NO, and boundary layer depths, Atmos Pollut Res, 7, 66–74, https://doi.org/10.1016/j.apr.2015.07.006, 2016.

Cazorla, M.: Ozone structure over the equatorial Andes from balloon-borne observations and zonal connection with two tropical sea level sites, J Atmos Chem, 74, 377–398, https://doi.org/10.1007/s10874-016-9348-2, 2017.

Cazorla, M. and Herrera, E.: An ozonesonde evaluation of spaceborne observations in the Andean tropics, Sci Rep, 12, 15942, https://doi.org/10.1038/s41598-022-20303-7, 2022a.

Cazorla, M. and Herrera, E.: An ozonesonde evaluation of spaceborne observations in the Andean tropics, Sci Rep, 12, 15942, https://doi.org/10.1038/s41598-022-20303-7, 2022b.

https://doi.org/10.5194/egusphere-2024-3720
Preprint. Discussion started: 19 December 2024

Cazorla, M. and Juncosa, J.: Planetary boundary layer evolution over an equatorial Andean valley: A simplified model based on balloon-borne and surface measurements, Atmospheric Science Letters, 19, e829, https://doi.org/10.1002/asl.829, 2018.

Cazorla, M., Brune, W. H., Ren, X., and Lefer, B.: Direct measurement of ozone production rates in Houston in 2009 and comparison with two estimation methods, Atmos Chem Phys, 12, 1203–1212, https://doi.org/10.5194/acp-12-1203-2012, 2012.

Cazorla, M., Parra, R., Herrera, E., and da Silva, F. R.: Characterizing ozone throughout the atmospheric column over the tropical Andes from in situ and remote sensing observations, Elementa: Science of the Anthropocene, 9, https://doi.org/10.1525/elementa.2021.00019, 2021a.

Cazorla, M., Herrera, E., Palomeque, E., and Saud, N.: What the COVID-19 lockdown revealed about photochemistry and ozone production in Quito, Ecuador, Atmos Pollut Res, 12, 124–133, https://doi.org/10.1016/j.apr.2020.08.028, 2021b.

Cazorla, M., Gallardo, L., and Jimenez, R.: The complex Andes region needs improved efforts to face climate extremes, Elementa, 10, https://doi.org/10.1525/elementa.2022.00092, 2022.

Cazorla, M., Giles, D. M., Herrera, E., Suárez, L., Estevan, R., Andrade, M., and Bastidas, Á.: Latitudinal and temporal distribution of aerosols and precipitable water vapor in the tropical Andes from AERONET, sounding, and MERRA-2 data, Sci Rep, 14, 897, https://doi.org/10.1038/s41598-024-51247-9, 2024.

Checa-Garcia, R., Hegglin, M. I., Kinnison, D., Plummer, D. A., and Shine, K. P.: Historical Tropospheric and Stratospheric Ozone Radiative Forcing Using the CMIP6 Database, Geophys Res Lett, 45, 3264–3273, https://doi.org/10.1002/2017GL076770, 2018.

Dusanter, S., Vimal, D., Stevens, P. S., Volkamer, R., Molina, L. T., Baker, A., Meinardi, S., Blake, D., Sheehy, P., Merten, A., Zhang, R., Zheng, J., Fortner, E. C., Junkermann, W., Dubey, M., Rahn, T., Eichinger, B., Lewandowski, P., Prueger, J., and Holder, H.: Measurements of OH and HO₂ concentrations during the MCMA-2006 field campaign – Part 2: Model comparison and radical budget, Atmos Chem Phys, 9, 6655–6675, https://doi.org/10.5194/acp-9-6655-2009, 2009.

Elshorbany, Y. F., Kurtenbach, R., Wiesen, P., Lissi, E., Rubio, M., Villena, G., Gramsch, E., Rickard, A. R., Pilling, M. J., and Kleffmann, J.: Oxidation capacity of the city air of Santiago, Chile, Atmos Chem Phys, 9, 2257–2273, https://doi.org/10.5194/acp-9-2257-2009, 2009a.

Elshorbany, Y. F., Kleffmann, J., Kurtenbach, R., Rubio, M., Lissi, E., Villena, G., Gramsch, E., Rickard, A. R., Pilling, M. J., and Wiesen, P.: Summertime photochemical ozone formation in Santiago, Chile, Atmos Environ, 43, 6398–6407, https://doi.org/10.1016/j.atmosenv.2009.08.047, 2009b.

Fanizza, C., Incoronato, F., Baiguera, S., Schiro, R., and Brocco, D.: Volatile organic compound levels at one site in Rome urban air, Atmos Pollut Res, 5, 303–314, https://doi.org/10.5094/APR.2014.036, 2014.

Gallardo, L., Olivares, G., Langner, J., and Aarhus, B.: Coastal lows and sulfur air pollution in Central Chile, Atmos Environ, 36, 3829–3841, https://doi.org/10.1016/S1352-2310(02)00285-6, 2002.

Garreaud, RenéD., Rutllant, JoséA., and Fuenzalida, H.: Coastal Lows along the Subtropical West Coast of South America: Mean Structure and Evolution, Mon Weather Rev, 130, 75–88, https://doi.org/10.1175/1520-0493(2002)130<0075:CLATSW>2.0.CO;2, 2002.

Gery, M. W., Whitten, G. Z., Killus, J. P., and Dodge, M. C.: A photochemical kinetics mechanism for urban and regional scale computer modeling, Journal of Geophysical Research: Atmospheres, 94, 12925–12956, https://doi.org/10.1029/JD094iD10p12925, 1989.

Global Modeling and Assimilation Office (GMAO): tavg1_2d_rad_Nx: MERRA-2 2D, time series area-averaged surface albedo, time average hourly (0.5x0.625), version 5.12.4, Greenbelt, MD, USA: Goddard Space Flight Center Distributed Active Archive Center (GSFC DAAC), Accessed February 2023 at doi: 10.5067/Q9QMY5PBNV1T., 2015a.

Global Modeling and Assimilation Office (GMAO): tavg1_2d_slv_Nx: MERRA-2 2D, time series area-averaged total column ozone, time average hourly (0.5x0.625), version 5.12.4, Greenbelt, MD, USA: Goddard Space Flight Center Distributed Active Archive Center (GSFC DAAC), Accessed February 2023 at doi: 10.5067/VJAFPLI1CSIV, 2015b.

https://doi.org/10.5194/egusphere-2024-3720
Preprint. Discussion started: 19 December 2024

Gómez Peláez, L. M., Santos, J. M., de Almeida Albuquerque, T. T., Reis, N. C., Andreão, W. L., and de Fátima Andrade, M.: Air quality status and trends over large cities in South America, Environ Sci Policy, 114, 422–435, https://doi.org/10.1016/j.envsci.2020.09.009, 2020.

Haagen-Smit, A. J. and Fox, M. M.: Ozone Formation in Photochemical Oxidation of Organic Substances, Ind Eng Chem, 48, 1484–1487, https://doi.org/10.1021/ie51400a033, 1956.

Huneeus, N., Gallardo, L., and Rutllant, J. A.: Offshore transport episodes of anthropogenic sulfur in northern Chile: Potential impact on the stratocumulus cloud deck, Geophys Res Lett, 33, https://doi.org/10.1029/2006GL026921, 2006.

Intergovernmental Panel on Climate Change (IPCC): Short-lived Climate Forcers. In: Climate Change 2021 – The Physical Science Basis: Working Group I Contribution to the Sixth Assessment Report of the Intergovernmental Panel on Climate Change, in: Climate Change 2021 – The Physical Science Basis, Cambridge University Press, 817–922, https://doi.org/10.1017/9781009157896.008, 2023.

Jaimes-Palomera, M., Retama, A., Elias-Castro, G., Neria-Hernández, A., Rivera-Hernández, O., and Velasco, E.: Non-methane hydrocarbons in the atmosphere of Mexico City: Results of the 2012 ozone-season campaign, Atmos Environ, 132, 258–275, https://doi.org/10.1016/j.atmosenv.2016.02.047, 2016.

Jenkin, M. E., Saunders, S. M., and Pilling, M. J.: The tropospheric degradation of volatile organic compounds: a protocol for mechanism development, Atmos Environ, 31, 81–104, https://doi.org/10.1016/S1352-2310(96)00105-7, 1997.

Jenkin, M. E., Saunders, S. M., Wagner, V., and Pilling, M. J.: Protocol for the development of the Master Chemical Mechanism, MCM v3 (Part B): tropospheric degradation of aromatic volatile organic compounds, Atmos Chem Phys, 3, 181–193, https://doi.org/10.5194/acp-3-181-2003, 2003.

Jenkin, M. E., Young, J. C., and Rickard, A. R.: The MCM v3.3.1 degradation scheme for isoprene, Atmos Chem Phys, 15, 11433–11459, https://doi.org/10.5194/acp-15-11433-2015, 2015.

Karlsson, P. E., Klingberg, J., Engardt, M., Andersson, C., Langner, J., Karlsson, G. P., and Pleijel, H.: Past, present and future concentrations of ground-level ozone and potential impacts on ecosystems and human health in northern Europe, Science of The Total Environment, 576, 22–35, https://doi.org/10.1016/j.scitotenv.2016.10.061, 2017.

Kleinman, L. I.: The dependence of tropospheric ozone production rate on ozone precursors, Atmos Environ, 39, 575–586, https://doi.org/10.1016/j.atmosenv.2004.08.047, 2005a.

Kleinman, L. I.: The dependence of tropospheric ozone production rate on ozone precursors, Atmos Environ, 39, 575–586, https://doi.org/10.1016/j.atmosenv.2004.08.047, 2005b.

Kleinman, L. I., Daum, P. H., Lee, Y., Nunnermacker, L. J., Springston, S. R., Weinstein-Lloyd, J., and Rudolph, J.: Sensitivity of ozone production rate to ozone precursors, Geophys Res Lett, 28, 2903–2906, https://doi.org/10.1029/2000GL012597, 2001a.

Kleinman, L. I., Daum, P. H., Lee, Y., Nunnermacker, L. J., Springston, S. R., Weinstein-Lloyd, J., and Rudolph, J.: Sensitivity of ozone production rate to ozone precursors, Geophys Res Lett, 28, 2903–2906, https://doi.org/10.1029/2000GL012597, 2001b.

Levy, H.: Normal Atmosphere: Large Radical and Formaldehyde Concentrations Predicted, Science (1979), 173, 141–143, https://doi.org/10.1126/science.173.3992.141, 1971.

Logan, J. A., Prather, M. J., Wofsy, S. C., and McElroy, M. B.: Tropospheric chemistry: A global perspective, J Geophys Res Oceans, 86, 7210–7254, https://doi.org/10.1029/JC086iC08p07210, 1981.

Lyu, X., Li, K., Guo, H., Morawska, L., Zhou, B., Zeren, Y., Jiang, F., Chen, C., Goldstein, A. H., Xu, X., Wang, T., Lu, X., Zhu, T., Querol, X., Chatani, S., Latif, M. T., Schuch, D., Sinha, V., Kumar, P., Mullins, B., Seguel, R., Shao, M., Xue, L., Wang, N., Chen, J., Gao, J., Chai, F., Simpson, I., Sinha, B., and Blake, D. R.: A synergistic ozone-climate control to address emerging ozone pollution challenges, https://doi.org/10.1016/j.oneear.2023.07.004, 2023.

Madden, M. C. and Hogsett, W. E.: A Historical Overview of the Ozone Exposure Problem, Human and Ecological Risk Assessment: An International Journal, 7, 1121–1131, https://doi.org/10.1080/20018091094880, 2001.

Malley, C. S., Henze, D. K., Kuylenstierna, J. C. I., Vallack, H. W., Davila, Y., Anenberg, S. C., Turner, M. C., and Ashmore, M. R.: Updated Global Estimates of Respiratory Mortality in Adults ≥30Years of Age Attributable to Long-Term Ozone Exposure, Environ Health Perspect, 125, https://doi.org/10.1289/EHP1390, 2017.

https://doi.org/10.5194/egusphere-2024-3720
Preprint. Discussion started: 19 December 2024

Mills, G., Harmens, H., Wagg, S., Sharps, K., Hayes, F., Fowler, D., Sutton, M., and Davies, B.: Ozone impacts on vegetation in a nitrogen enriched and changing climate, Environmental Pollution, 208, 898–908, https://doi.org/10.1016/j.envpol.2015.09.038, 2016.

Muñoz, L. E., Campozano, L. V., Guevara, D. C., Parra, R., Tonato, D., Suntaxi, A., Maisincho, L., Páez, C., Villacís, M., Córdova, J., and Valencia, N.: Comparison of Radiosonde Measurements of Meteorological Variables with Drone, Satellite Products, and WRF Simulations in the Tropical Andes: The Case of Quito, Ecuador, Atmosphere (Basel), 14, 264, https://doi.org/10.3390/atmos14020264, 2023.

Muñoz, R. C. and Undurraga, A. A.: Daytime Mixed Layer over the Santiago Basin: Description of Two Years of Observations with a Lidar Ceilometer, J Appl Meteorol Climatol, 49, 1728–1741, https://doi.org/10.1175/2010JAMC2347.1, 2010.

Osses, A., Gallardo, L., and Faundez, T.: Analysis and evolution of air quality monitoring networks using combined statistical information indexes, Tellus B: Chemical and Physical Meteorology, 65, 19822, https://doi.org/10.3402/tellusb.v65i0.19822, 2013.

Pagonis, D., Sekimoto, K., and de Gouw, J.: A Library of Proton-Transfer Reactions of H_3O^+ Ions Used for Trace Gas Detection, J Am Soc Mass Spectrom, 30, 1330–1335, https://doi.org/10.1007/s13361-019-02209-3, 2019.

Parra, R. and Espinoza, C.: Insights for Air Quality Management from Modeling and Record Studies in Cuenca, Ecuador, Atmosphere (Basel), 11, 998, https://doi.org/10.3390/atmos11090998, 2020.

Ren, X., van Duin, D., Cazorla, M., Chen, S., Mao, J., Zhang, L., Brune, W. H., Flynn, J. H., Grossberg, N., Lefer, B. L., Rappenglück, B., Wong, K. W., Tsai, C., Stutz, J., Dibb, J. E., Thomas Jobson, B., Luke, W. T., and Kelley, P.: Atmospheric oxidation chemistry and ozone production: Results from SHARP 2009 in Houston, Texas, Journal of Geophysical Research: Atmospheres, 118, 5770–5780, https://doi.org/10.1002/jgrd.50342, 2013.

Saunders, S. M., Jenkin, M. E., Derwent, R. G., and Pilling, M. J.: Protocol for the development of the Master Chemical Mechanism, MCM v3 (Part A): tropospheric degradation of non-aromatic volatile organic compounds, Atmos Chem Phys, 3, 161–180, https://doi.org/10.5194/acp-3-161-2003, 2003.

Saunier, A., Ormeño, E., Piga, D., Armengaud, A., Boissard, C., Lathière, J., Szopa, S., Genard-Zielinski, A.-C., and Fernandez, C.: Isoprene contribution to ozone production under climate change conditions in the French Mediterranean area, Reg Environ Change, 20, 111, https://doi.org/10.1007/s10113-020-01697-4, 2020.

Sebol, A. E., Canty, T. P., Wolfe, G. M., Hannun, R., Ring, A. M., and Ren, X.: Exploring ozone production sensitivity to NOx and VOCs in the New York City airshed in the spring and summers of 2017–2019, Atmos Environ, 324, 120417, https://doi.org/10.1016/j.atmosenv.2024.120417, 2024.

Seguel, R. J., Gallardo, L., Fleming, Z. L., and Landeros, S.: Two decades of ozone standard exceedances in Santiago de Chile, Air Qual Atmos Health, 13, 593–605, https://doi.org/10.1007/s11869-020-00822-w, 2020.

Seguel, R. J., Gallardo, L., Osses, M., Rojas, N. Y., Nogueira, T., Menares, C., de Fatima Andrade, M., Belalcázar, L. C., Carrasco, P., Eskes, H., Fleming, Z. L., Huneeus, N., Ibarra-Espinosa, S., Landulfo, E., Leiva, M., Mangones, S. C., Morais, F. G., Moreira, G. A., Pantoja, N., Parraguez, S., Rojas, J. P., Rondanelli, R., da Silva Andrade, I., Toro, R., and Yoshida, A. C.: Photochemical sensitivity to emissions and local meteorology in Bogotá, Santiago, and São Paulo, Elementa: Science of the Anthropocene, 10, https://doi.org/10.1525/elementa.2021.00044, 2022.

Seguel, R. J., Castillo, L., Opazo, C., Rojas, N. Y., Nogueira, T., Cazorla, M., Gavidia-Calderón, M., Gallardo, L., Garreaud, R., Carrasco-Escaff, T., and Elshorbany, Y.: Changes in South American surface ozone trends: exploring the influences of precursors and extreme events, Atmos Chem Phys, 24, 8225–8242, https://doi.org/10.5194/acp-24-8225-2024, 2024.

Seinfeld, J. H. and Pandis, S. N.: Atmospheric Chemistry and Physics: From Air Pollution to Climate Change, John Wiley & Sons, Hoboken, NJ, USA, 2016.

Shirley, T. R., Brune, W. H., Ren, X., Mao, J., Lesher, R., Cardenas, B., Volkamer, R., Molina, L. T., Molina, M. J., Lamb, B., Velasco, E., Jobson, T., and Alexander, M.: Atmospheric oxidation in the Mexico City Metropolitan Area (MCMA) during April 2003, Atmos Chem Phys, 6, 2753–2765, https://doi.org/10.5194/acp-6-2753-2006, 2006.

Sillman, S.: The use of NO_y, H_2O_2, and HNO_3 as indicators for ozone-NO_x-hydrocarbon sensitivity in urban locations, Journal of Geophysical Research: Atmospheres, 100, 14175–14188, https://doi.org/10.1029/94JD02953, 1995.

https://doi.org/10.5194/egusphere-2024-3720
Preprint. Discussion started: 19 December 2024

Soares, A. R. and Silva, C.: Review of Ground-Level Ozone Impact in Respiratory Health Deterioration for the Past Two Decades, Atmosphere (Basel), 13, 434, https://doi.org/10.3390/atmos13030434, 2022.

Sokhi, R. S., Singh, V., Querol, X., Finardi, S., Targino, A. C., Andrade, M. de F., Pavlovic, R., Garland, R. M., Massagué, J., Kong, S., Baklanov, A., Ren, L., Tarasova, O., Carmichael, G., Peuch, V. H., Anand, V., Arbilla, G., Badali, K., Beig, G., Belalcazar, L. C., Bolignano, A., Brimblecombe, P., Camacho, P., Casallas, A., Charland, J. P., Choi, J., Chourdakis, E., Coll, I., Collins, M., Cyrys, J., da Silva, C. M., Di Giosa, A. D., Di Leo, A., Ferro, C., Gavidia-Calderon, M., Gayen, A., Ginzburg, A., Godefroy, F., Gonzalez, Y. A., Guevara-Luna, M., Haque, S. M., Havenga, H., Herod, D., Hõrrak, U., Hussein, T., Ibarra, S., Jaimes, M., Kaasik, M., Khaiwal, R., Kim, J., Kousa, A., Kukkonen, J., Kulmala, M., Kuula, J., La Violette, N., Lanzani, G., Liu, X., MacDougall, S., Manseau, P. M., Marchegiani, G., McDonald, B., Mishra, S. V., Molina, L. T., Mooibroek, D., Mor, S., Moussiopoulos, N., Murena, F., Niemi, J. V., Noe, S., Nogueira, T., Norman, M., Pérez-Camaño, J. L., Petäjä, T., Piketh, S., Rathod, A., Reid, K., Retama, A., Rivera, O., Rojas, N. Y., Rojas-Quincho, J. P., San José, R., Sánchez, O., Seguel, R. J., Sillanpää, S., Su, Y., Tapper, N., Terrazas, A., Timonen, H., Toscano, D., Tsegas, G., Velders, G. J. M., Vlachokostas, C., von Schneidemesser, E., VPM, R., Yadav, R., Zalakeviciute, R., and Zavala, M.: A global observational analysis to understand changes in air quality during exceptionally low anthropogenic emission conditions, Environ Int, 157, https://doi.org/10.1016/j.envint.2021.106818, 2021.

Thornton, J. A., Wooldridge, P. J., Cohen, R. C., Martinez, M., Harder, H., Brune, W. H., Williams, E. J., Roberts, J. M., Fehsenfeld, F. C., Hall, S. R., Shetter, R. E., Wert, B. P., and Fried, A.: Ozone production rates as a function of NO_x abundances and HO_x production rates in the Nashville urban plume, Journal of Geophysical Research: Atmospheres, 107, https://doi.org/10.1029/2001JD000932, 2002a.

Thornton, J. A., Wooldridge, P. J., Cohen, R. C., Martinez, M., Harder, H., Brune, W. H., Williams, E. J., Roberts, J. M., Fehsenfeld, F. C., Hall, S. R., Shetter, R. E., Wert, B. P., and Fried, A.: Ozone production rates as a function of NO_x abundances and HO_x production rates in the Nashville urban plume, Journal of Geophysical Research: Atmospheres, 107, https://doi.org/10.1029/2001JD000932, 2002b.

Wolfe, G. M., Marvin, M. R., Roberts, S. J., Travis, K. R., and Liao, J.: The Framework for 0-D Atmospheric Modeling (F0AM) v3.1, Geosci Model Dev, 9, 3309–3319, https://doi.org/10.5194/gmd-9-3309-2016, 2016.

Zhang, Y., Han, Z., Li, X., Zhang, H., Yuan, X., Feng, Z., Wang, P., Mu, Z., Song, W., Blake, D. R., Ying, Q., George, C., Sheng, G., Peng, P., and Wang, X.: Plants and related carbon cycling under elevated ground-level ozone: A mini review, Applied Geochemistry, 144, 105400, https://doi.org/10.1016/j.apgeochem.2022.105400, 2022.